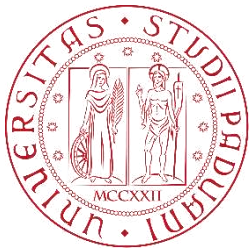

UNIVERSITÀ DEGLI STUDI DI PAVOVA

Department of Land, Environment Agriculture and Forestry

Second Cycle Degree (MSc)

In Forest Science

Using X-ray tomography to investigate species-specific colonization patterns of ambrosia beetles in flooded trees

Supervisor

Dr. Davide Rassati

Co-supervisor

Dr. Giacomo Santoiemma

Submitted by

Elia Scabbio

Student n. 2027874

ACADEMIC YEAR 2022 – 2023

ABSTRACT

This study employs X-ray tomography to explore species-specific colonization patterns of ambrosia beetles in flooded trees. The research focuses on elucidating the impact of tree species on host selection and colonization success among ambrosia beetles under simulated flooding conditions. The investigation compares the variations in the number of entry holes (a proxy for host selection) and the number of successful galleries (a proxy for colonization success) across eight distinct tree species prevalent in orchard and forest ecosystems. The species investigated include *Malus sylvestris*, *Prunus armeniaca*, *Prunus avium*, *Pyrus pyraster*, *Corylus avellana*, *Carpinus betulus*, *Quercus ilex*, and *Quercus robur*.

The results highlight the indispensable role of ethanol in the plant-host relationship, influencing both host selection mechanisms and colonization success of four species of ambrosia beetles: *Xylosandrus crassiusculus*, *Xylosandrus germanus*, *Xyleborinus saxesenii* and *Anisandrus dispar*. The study reveals differential effects of flooding stress on these ambrosia beetle species boring activities and colonization success, with trees in the Rosales group being subjected to higher attack frequencies and higher colonization success levels than those in the Fagales group.

Furthermore, the research emphasizes the potential threat of ambrosia beetles in orchards and nurseries, in particularly *Xylosandrus crassiusculus* was proven to be highly adaptable to different conditions and tree species, thus posing a potential threat for trees that are undergoing flooding stress. As climate change increases the frequency of flooding events worldwide, understanding ambrosia beetle behaviour becomes crucial for effective monitoring and pest management in both managed and natural environments.

Table of Contents

1. INTRODUCTION

1.1. Ecology of Ambrosia beetles

The term “ambrosia beetles” encompasses a diverse ecological strategy shared among thousands of wood-boring weevil species (Coleoptera: Curculionidae), including about 6,000 species found globally across over 250 genera (Hulcr & Skelton, 2023; Faccoli 2015). Ambrosia beetles are members of two weevil subfamilies, Scolytinae and Platypodinae, which share a common ecological strategy: fungus farming. These beetles introduce symbiotic fungi within their tunnels to let them colonize the gallery, thus establishing fungus gardens from which the insects harvest food sources for both the adults and their offspring. (Dzurenko & Hulcr, 2022; Hulcr & Skelton, 2023).

Ambrosia beetles are among the smallest weevils, with most species below 5 mm and always less than one centimetre in length (Fig 1.1). They possess short legs and antennas, and an elongated and cylindrical body adapted for boring into the wood and navigating inside tunnels, typically dark and shiny in colour, provided with strong jaws (Dzurenko & Hulcr, 2022; Faccoli, 2015; Hulcr et al., 2015).

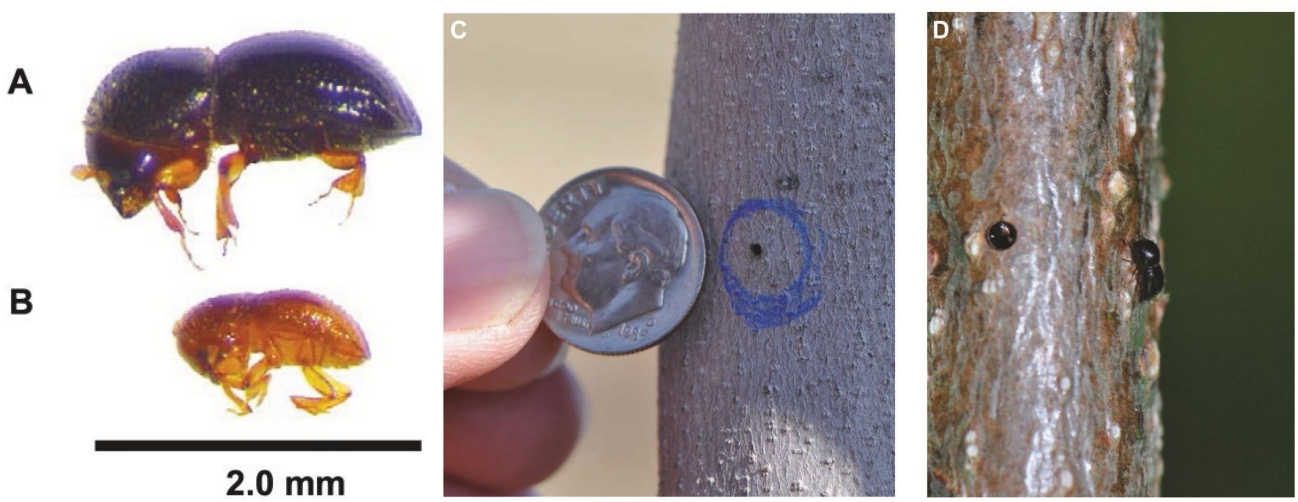

Figure 1.1. *Xylosandrus germanus* adult female (**A**) and male (**B**), the latter are also flightless. (**C**) The gallery entrance created by ambrosia beetles are generally around 1 mm in diameter. (**D**) An adult *X. germanus* and a gallery entrance created in sweetbay magnolia. (Source: Ranger et al., 2016. Photos by C. Ranger)

To start the colonization, adult female ambrosia beetles create an initial horizontal tunnel within the xylem, typically on the trunk or the stem, where they introduce the spores of the symbiont fungus. From this central tunnel, a network of additional tunnels may branch out, and some of them widen to form brood chambers, where eggs are deposited in the distal portion (Ranger et al., 2016a). The

larvae then relocate and commence their feeding on the fungus present within these galleries, sustaining themselves until they reach maturity (Hoffman, 1941).

Ambrosia beetles share a powerful ecological and evolutionary bond with their symbiotic fungi, being considered reciprocally obligate mutualists: these insects carry around the fungal spores in specialized anatomical structures on their exoskeletons called *mycangia*, that maintain, shelter, and nourish living fungal propagules in dormant and dispersing adult beetles (Dzurenko & Hulcr, 2022; Hulcr & Skelton, 2023; Batra, 1963; Skelton et al., 2019a) (Fig. 1.2).

Among the most well-known ambrosia fungi, many belong to the order Ophiostomatales, especially the genus *Raffaelea*. Some species exhibit high selectivity for their fungal symbiont, favouring only one or a few fungal species and excluding antagonistic fungal parasites and competitors (Skelton et al., 2019a; Hulcr & Skelton, 2023; Hulcr & Stelinsky, 2017). Conversely, others may carry spores of different fungal species in their mycangium, with Xyleborini in the Xyleborus group being among the most promiscuous, often carrying several species of *Raffaelea* (Hulcr & Stelinsky, 2017).

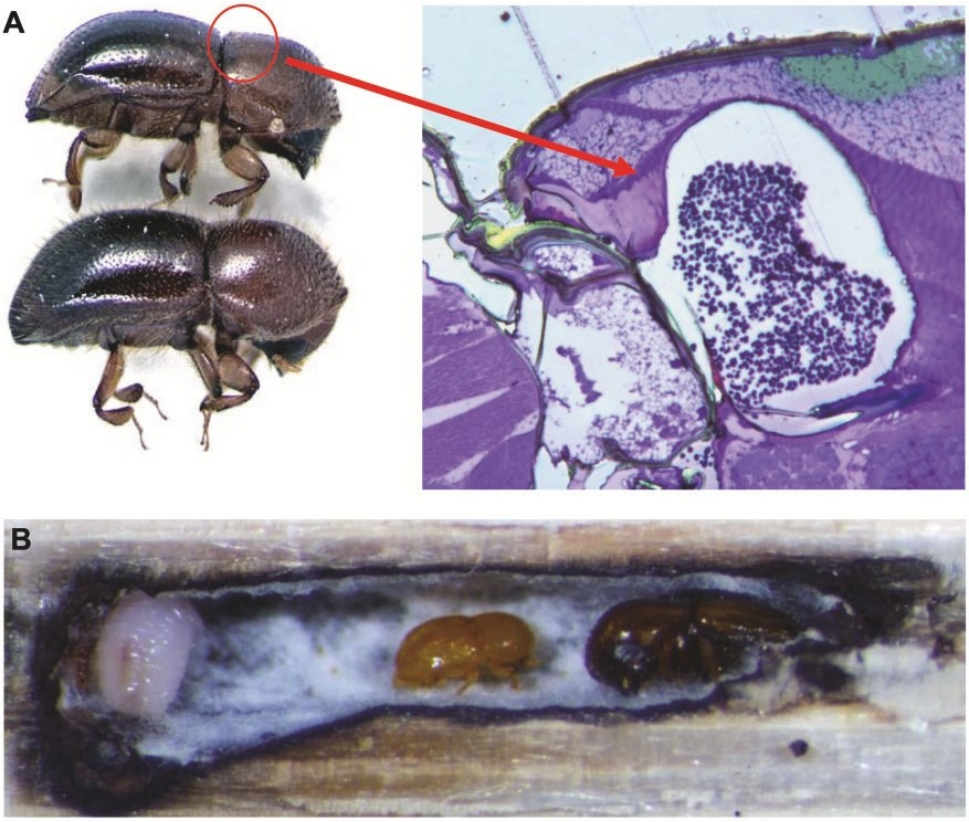

Figure 1.2. (**A**) In *X. germanus* and *crassiusculus*, spores of the symbiotic fungus are contained within the mycangium located between the pro- and mesothorax. (**B**) White ambrosial form of *X. germanus*' symbiotic fungus growing within a gallery containing a larvae, adult male, and adult female. (Source: Ranger et al., 2016. Photo 2A by B. Anderson and 2B by C. Ranger)

Despite the roles are shifting between host and symbiont during the beetle and fungus life cycle, being the insect the host of the fungus during its dispersion and then the fungi hosting the insect within the colonized gallery (Hulcr & Skelton, 2023), both partners derive benefits from this ambrosia symbiosis: the beetles gain sustenance from the fungi, while the fungi are dispersed to suitable habitats by the beetles (Dzurenko & Hulcr, 2022). Since ambrosia beetles bypass the plant's chemical defences by not feeding directly on host tissues, they can colonize a wide range of tree species and spend a substantial portion of their adult lives sheltered within woody tissues, safe from predators, parasitoids, and adverse environmental conditions (Hulcr & Skelton, 2023; Dzurenko & Hulcr, 2022; Kirkendall et al., 2015).

Within this stable and protected environment, ambrosia beetles primarily or exclusively feed on their fungal symbionts, which concentrate nutrients in enlarged conidia available to their larvae and newly emerged adults (Hulcr & Skelton, 2023; Dzurenko & Hulcr, 2022). These fungi may grow in different forms (Fig. 1.3), depending on the presence or absence of the beetles, thus providing adequate food sources for the development of larvae and pupae (Ranger et al., 2016a) and allowing the transmission of the symbiont fungi to the offspring through feeding (Carillo et al., 2013).

The ecology of the fungal mutualist has a direct effect on the degree of complexity of the beetle society: in large dead tree trunks, where the symbiotic *Raffaelea* spp. can persist long enough to support multiple life cycles, subsociality strategy among *Xyleborus* and *Xyleborinus* may lead to overlap of multiple developmental stages as well as a rich array of interactions, including allogrooming, cooperation in gallery maintenance, and disposal of debris (Hulcr & Stelinsky, 2017). Moreover, Xyleborini ambrosia beetles show high levels of inbreeding among siblings within the gallery system (Ranger et al., 2016a; Dzurenko & Hulcr, 2022).

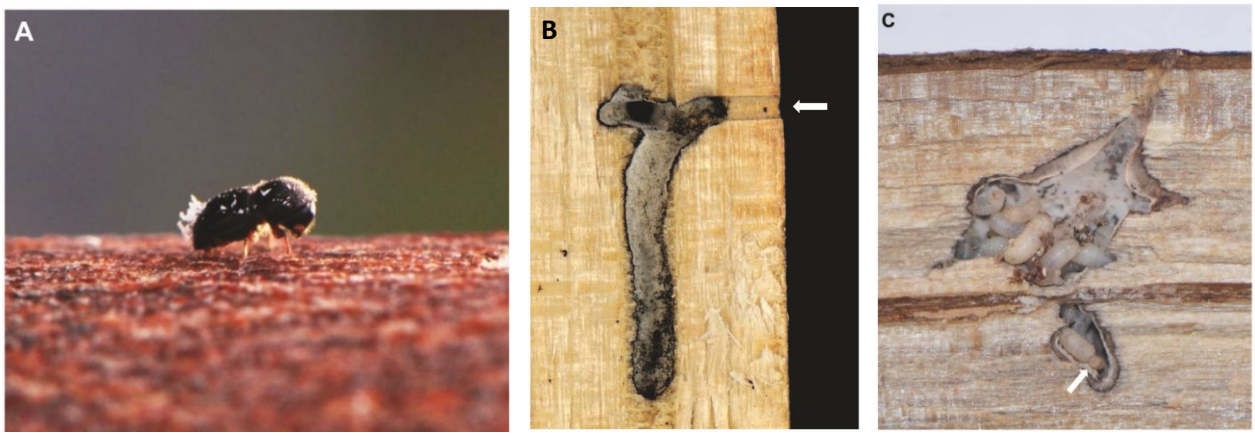

Figure 1.3. (**A**) An adult female *X. germanus* with fungal growths on her body. (**B-C**) Galleries with established fungal gardens, arrows indicate the entrance and the eggs. (Source: Ranger et al., 2016. Photos by C. Ranger)

1.2. Relationship with trees and host selection mechanism

Ambrosia beetles infest dead or stressed trees (Carillo et al., 2013; Hulcr & Stelinsky, 2017), exploiting their weakened state to colonize them. The majority of the species favour trees that are dead or nearly so, which no longer process functioning defensive mechanisms (Hulcr & Skelton, 2023; Hulcr & Stelinsky, 2017); however, some species specialize in attacking living hosts under stress conditions, becoming forest and silvicultural pests (Hulcr & Skelton, 2023; Hulcr et al., 2017; Ranger et al., 2015; Wang et al., 2021).

Ambrosia Beetles rely on chemical signals released by distressed or deceased trees as olfactory cues to select an appropriate host for colonization (Cavalletto et al., 2021; Ranger et al., 2010, 2012, 2015, 2021). Many different chemicals may attract or repel Ambrosia beetles, among which ethanol is an effective attractant for many different unrelated beetle species (Kamata et al., 2008; Ranger et al., 2010; Kendra et al., 2017) and has a key role in ambrosia beetles host selection mechanism.

Ethanol is induced and emitted by trees when stressed by abiotic factors, such as frost, flood, and drought (Kelsey et al., 2014; Copolovici & Niinemets, 2010; Ranger et al., 2013, 2016b, 2019; La Spina et al., 2013) or biotic factors, including the infection of trees by pathogens (Kelsey et al., 2013; McPherson et al., 2008). Among these, flooding is a major plant stress factor in many temperate countries in the Northern Hemisphere (Copolovici & Niinemets, 2010) and a recurrent condition on intensively managed trees, such as in ornamental plant nurseries and young orchards, and forests with poor soil drainage (Hulcr & Skelton, 2023; Ranger et al., 2016a) (Fig. 1.4A).

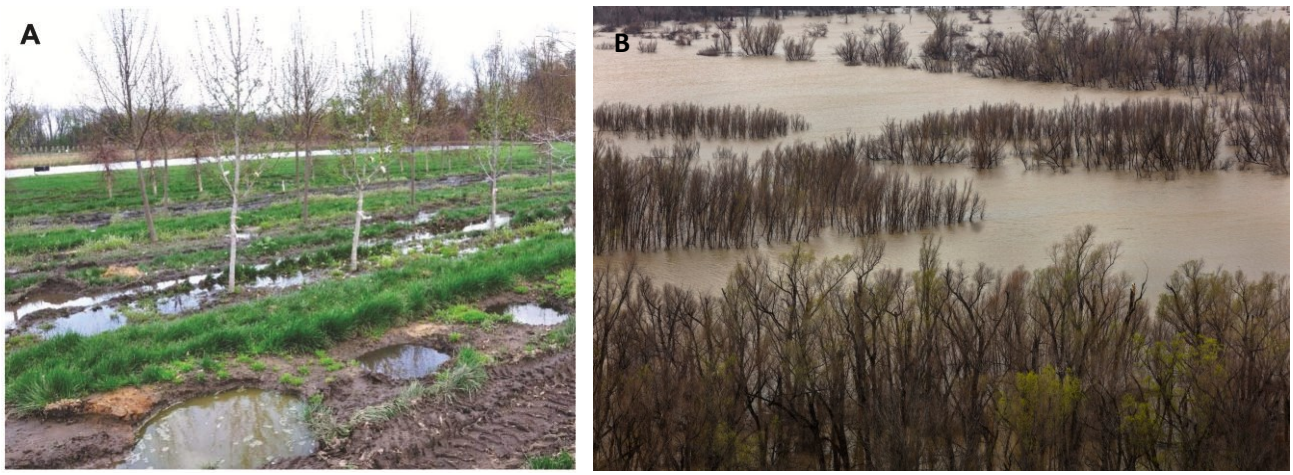

Figure 1.4. Trees subjected to flooding stress are more vulnerable to ambrosia beetles attacks. (**A**) An orchard subjected to flooding and poor drainage. (**B**) The Mississippi River overflowing its banks on February 28, 2020 in Vicksburg, Mississippi, flooding the nearby forest. (Source: photo 4A by C. Ranger from Ranger et al., 2016, photo 4B by Berry Lewis from Getty Images)

In addition, global change is inducing alterations in precipitation patterns and elevating sea levels, thereby enhancing flood stress risks in Northern Hemisphere temperate forests (Parry et al., 2007; Hulcr & Skelton, 2023; Easterling et al., 2000; Kharin & Zwiers, 2005), thus predisposing them to attacks by ambrosia beetles (Fig. 1.4B).

Copolovici and Niinemets (2010) analyze the effect of flooding on tree metabolism: a lower oxygen availability in the submerged plant part creates anoxic conditions in which a series of volatile stress marker compounds are produced and emitted, among which ethanol is converted from pyruvate formed during glycolysis and transported to the stem and leaf tissue (Ranger et al., 2012) (Fig. 1.5).

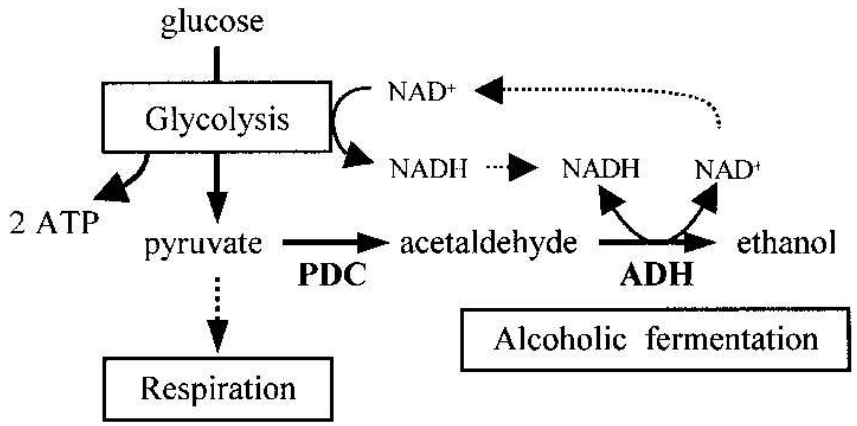

Figure 1.5. Diagram of alcoholic fermentation pathway in plants. Alcoholic fermentation occurs in anoxic conditions following two reaction steps: the decarboxylation of pyruvate to acetaldehyde by PDC and the subsequent reduction of acetaldehyde to ethanol by ADH. (Source: Mikio Nazakono from ResearchGate)

Rassati et al. (2020) and Cavalletto et al. (2021) discovered that ethanol concentration in tree tissues differentially affects the host selection of ambrosia beetles, and influences ecological niche partitioning among ambrosia beetle species, due to a broad host species range but a narrow preference based on the condition of the host (Rassati et al., 2020; Hulcr et al., 2007).

Ethanol also favours the growth of ambrosia beetles' nutritional fungal symbionts, as they can process ethanol and use it as a carbon source, whereas the antagonistic fungi are strongly inhibited in their growth by even small amounts of ethanol (Cavalletto et al., 2022; Lehenberger et al., 2021; Chen et al., 2021; Ranger et al., 2018).

Ranger et al. (2018) discovered that the colonization success of ambrosia beetles depends deeply on the capability of the symbiont fungus to establish flourishing fungal gardens. *Ambrosiella* and *Raffaelea* fungi can exploit and emit ethanol to maintain the selectivity of the environment to create favourable conditions. Oviposition is initiated only after the fungal gardens are established, thereby

posing a critical bottleneck in colonization success, brood production, and survivorship (Ranger et al., 2018; Chen et al., 2021).

Host selection mechanism is also influenced by the tree species, due to the emission of volatiles that enhance or inhibit the attraction of certain ambrosia beetles (Cavalletto et al., 2021; Rassati et al., 2016; Reding & Ranger, 2020).

Another way in which ambrosia beetle may cause the death of the attacked tree is through the inoculation of a virulent fungus partner, but this occurrence is restricted to *Xyleborus glabratus* which causes Laurel wilt, a deadly disease of susceptible trees in the Lauraceae caused by the fungus *Harringtonia lauricola* (Hulcr & Skelton, 2023; Hulcr & Stelinsky, 2017), and few other species.

However, the vast majority of ambrosia beetle species are harmless to forest environments, with minimal effects on human industries (Hulcr & Stelinsky, 2017), except for plant nurseries and orchards where the presence of these beetles may affect the ornamental value of the trees and make them not marketable (Hulcr & Skelton, 2023; Ranger et al., 2021) (Fig. 1.6).

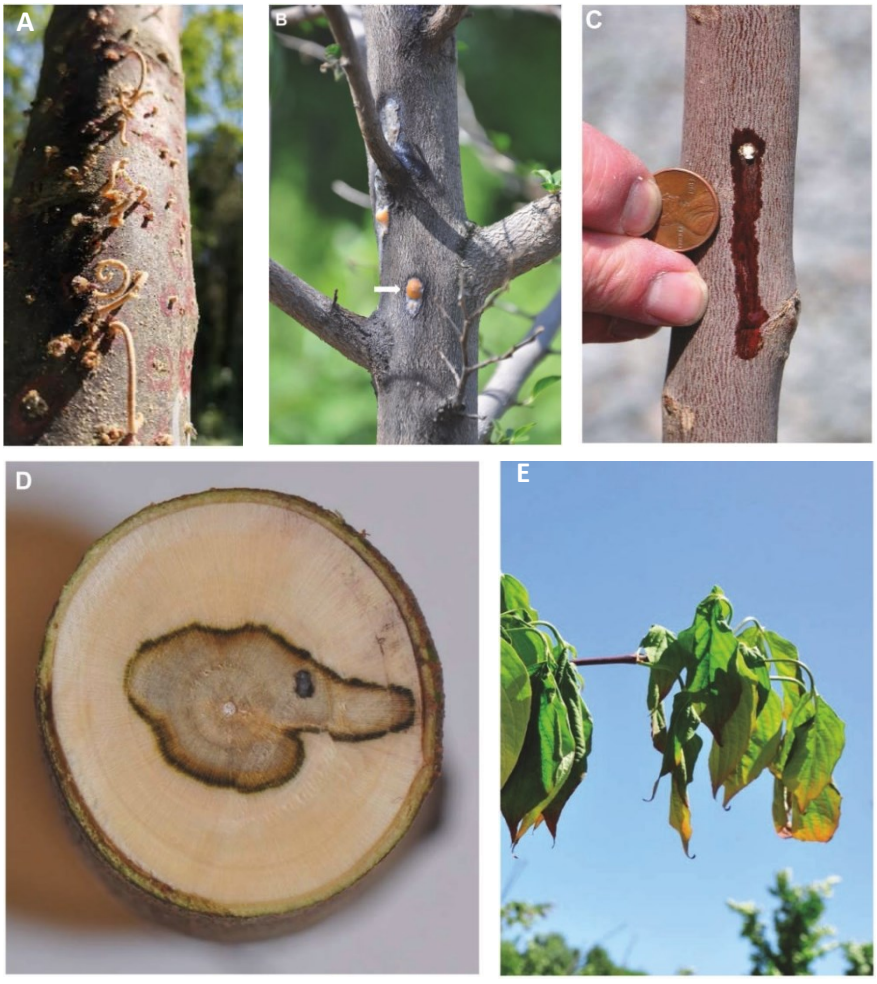

Figure 1.6. Ambrosia beetles dig their galleries through the bark, but the entrance hole may be difficult to spot due to their minute size. Other cues may indicate their presence inside the tree, such as (**A**) toothpick-like extrusion of wood, (**B**) presence of opportunistic pathogens exploiting the wound on the bark, (**C**) sap production around and below the hole, (**D**) wooden tissue discoloration or (**E**) wilting foliage during spring months. (Source: 6A from Carloni, 2022, 6B-E by C. Ranger from Ranger et al., 2016)

The management of ambrosia beetles aims towards maintaining plant health, as ambrosia beetles are poor colonizers of vigorous trees (Hulcr & Skelton, 2023; Hulcr & Stelinsky, 2017; Ranger et al., 2016b, 2020) and no biological and chemical control strategies have proven to be effective (Ranger et al., 2016b, 2020) (Fig. 1.7).

Hulcr and Skelton (2023) describe the ecological importance of ambrosia beetles: they often are the first colonizers of dead and dying trees in most forest ecosystems, and as such, they are likely to play an important role in the recycling of forest biomass and the release of carbon from decaying wood.

Skelton et al. (2019b, 2020) state that many of the saprotrophic fungi in decaying wood are introduced by ambrosia beetles and that some beetle-associated fungi exclude, or compete with, true wood-degrading fungi, resulting in decreased decay rates during the early stages of decomposition.

One of the foundational elements of modern forest entomology is that increased insect activity is a symptom of poor tree health (Manion, 1981; Hulcr & Skelton, 2023); rather than managing all ambrosia beetles strictly as pests, it may be more appropriate to consider many ambrosia beetle species as reliable bioindicators of underlying poor tree health that should be improved (Hulcr & Skelton, 2023).

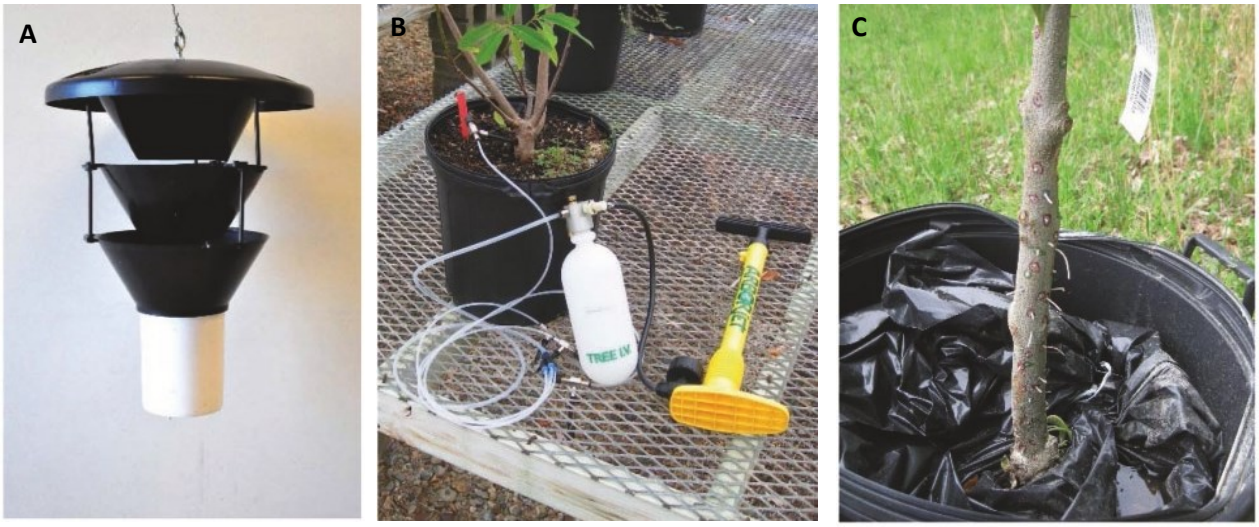

Figure 1.7. Management of ambrosia beetles in nurseries and orchards may be performed using traps, that attract the beetles and prevent the attacks on nearby trees. (**A**) Lindgren traps are commonly used in forestry, they can be purchased from a vendor and the number of funnels can be adjusted. (**B**) A tree can be injected with ethanol using a pressurized system to attract ambrosia beetles. (**C**) Trees intolerant to flooding can be flood-stressed and used as trap trees. (Source: from Ranger et al., 2016, photos by C. Ranger)

1.3. Influence of ethanol and host species on Xyleborini

Within the ambrosia beetle communities present in our territory, numerous species have become invasive beyond their native ranges, driven by globalization and international trade (Brockerhoff & Liebhold, 2017; Meurisse et al., 2019). Notably, the Xyleborini tribe has excelled as invaders (Rassati et al., 2016; Hulcr & Stelinski, 2017).

Species such as the Asian *Xylosandrus germanus* (Blandford) and *Xylosandrus crassiusculus* (Motschulsky), the Palaearctic *Anisandrus dispar* (Fabricius), and *Xyleborinus saxesenii* (Ratzeburg) are noteworthy examples. They pose threats not only in ornamental nurseries and orchards within their native and introduced regions but also exhibit the capacity to infest a wide array of tree species in forests, plantations, and woodlands (Galko et al., 2019; Ranger et al., 2015a, 2016a; Rassati et al., 2020).

Previous studies have established that the aforementioned ambrosia beetle species exhibit an affinity for ethanol presence in woody tissues (Rassati et al., 2020; Ranger et al., 2010), but Cavalletto et al. (2021, 2022) discovered how varying ethanol concentrations affect differently host selection and colonization success.

A. dispar (Fig. 1.8) has shown an attraction to increasing ethanol concentration (Klimetzek et al., 1986; Schroeder & Lindelöw, 1989), possibly due to the habit of this beetle of colonizing dying or decaying trees (Cavalletto et al., 2021). The symbiont fungi associated with this species is *Ambrosiella hartigii*, which favours an ethanol-rich environment (Lehenberger et al., 2021) and grants higher colonization success with increasing ethanol concentration (Cavalletto et al., 2022).

Figure 1.8. *A. dispar*, lateral and dorsal view. (Source: photo by J. Hulcr, from Xyleborini Ambrosia Beetles)

The host selection mechanism and colonization success in *X. saxesenii* (Fig. 1.9) are affected positively by an increasing ethanol concentration (Cavalleto et al., 2022; Rassati et al., 2020), and show a clear preference for certain tree species over others (Cavalletto et al., 2022; Chen et al., 2021; Yang et al., 2018; Owens et al., 2019), probably due to its symbiont fungi, *Raffaelea canadiensis*, being more sensitive to host-derived compounds over than ethanol (Cavalletto et al., 2021).

Figure 1.9. *X. saxesenii*, lateral and dorsal view. (Source: photo by J. Hulcr, from Xyleborini Ambrosia Beetles)

X. germanus (Fig. 1.10) and *X. crassiusculus* (Fig. 1.11) are known to have a broad host range, combined with haplodiploid reproduction, which makes them efficient colonizers (Kirkendall et al., 1993; Normark et al., 1999; Dole et al., 2010; Ranger et al., 2015b, 2016). Their fungal symbiont, respectively *Ambrosiella grosmanniae* and *Ambrosiella roeperi*, can grow at lower ethanol concentrations, making them able to colonize trees with lower stress levels (Ranger et al., 2018, 2016; Rassati et al., 2020). However, Cavalletto et al. (2022) show that *X. germanus* initiate boring at higher ethanol concentration.

Figure 1.10. *X. crassiusculus*, lateral and dorsal view. (Source: photo by J. Hulcr, from Xyleborini Ambrosia Beetles)

Figure 1.11. *X. germanus*, lateral and dorsal view. (Source: photo by J. Hulcr, from Xyleborini Ambrosia Beetles)

Rassati et al. (2020) and Cavalletto et al. (2021) support the theory of a niche-partitioning mechanism driven by ethanol concentration and host tree species, in determining the ecological niche of each insect species. Cavalletto et al. (2022) also showed that the optimal ethanol concentration maximizing colonization and offspring production can vary among species.

However, whether and how the host tree species is able to influence colonization patterns and host selection mechanism, remains unclear. Sensitivity or intolerance to flood stress in plants has been proven to influence positively host selection among ambrosia beetles (Ranger et al., 2015b), as higher stress levels raise the concentration of emitted ethanol.

Moreover, conflicting patterns have been observed for *A. dispar* and *X. germanus* in Cavalletto et al. (2022) when confronted with previous studies (Ranger et al., 2015b, 2016, 2018; Rassati et al., 2016, 2020; Cavalletto et al., 2021), which require more in-depth studies to be clarified.

Again, in Cavalletto et al. (2022), *X. crassiusculus* and *A. dispar* were proven to be more driven by ethanol concentration for boring initiation and colonization success than *X. saxesenii* and *X. germanus*, hypothesizing for the latter two species that volatiles other than ethanol could influence host selection (Yang et al., 2018; Chen et al., 2021).

1.4. Application of X-ray tomography in insect ecology

X-ray computer tomography (CT) is a useful and reliable technique that has become frequently used in insect-related studies (Alba-Alejandre et al., 2018), enabling the observation and monitoring of the cryptic lifestyles of wood-boring beetles.

This technology has been used on insects and invertebrates since the early 2000s (Postnov et al., 2002; Tarver et al., 2006; Nahirney et al., 2006), but the first application for wood-boring insects was performed on termites (Fuchs et al., 2004), reconstructing 3D images of the full structure of galleries inside the wood.

Many other studies, in which CT was applied to xylophagous and wood-boring insects, have followed (Jenning & Austin, 2011; Himmi et al. 2014, 2016a, 2016b, 2018; Aguilera-Olivares et al., 2017; Choi et al., 2017; Berville & Darrouzet, 2019; Harit et al. 2021; Donkò et al., 2022; Yang et al., 2022), aiming to a deeper comprehension of the habits, social behaviour, and life cycles of the insects through non-disruptive and advanced techniques (Fig. 1.12).

However, no studies on ambrosia beetles, that take advantage of CT, have been produced. The application of X-ray tomography to study the complex gallery networks of this group of insects has already been suggested by Alba-Alejandre et al. (2018), and a set of algorithms was presented by Dolinko et al. (2022) to facilitate recognition and volume estimation of each gallery for ambrosia beetles. Similar strategies have already been used in other studies (Seibold et al., 2022).

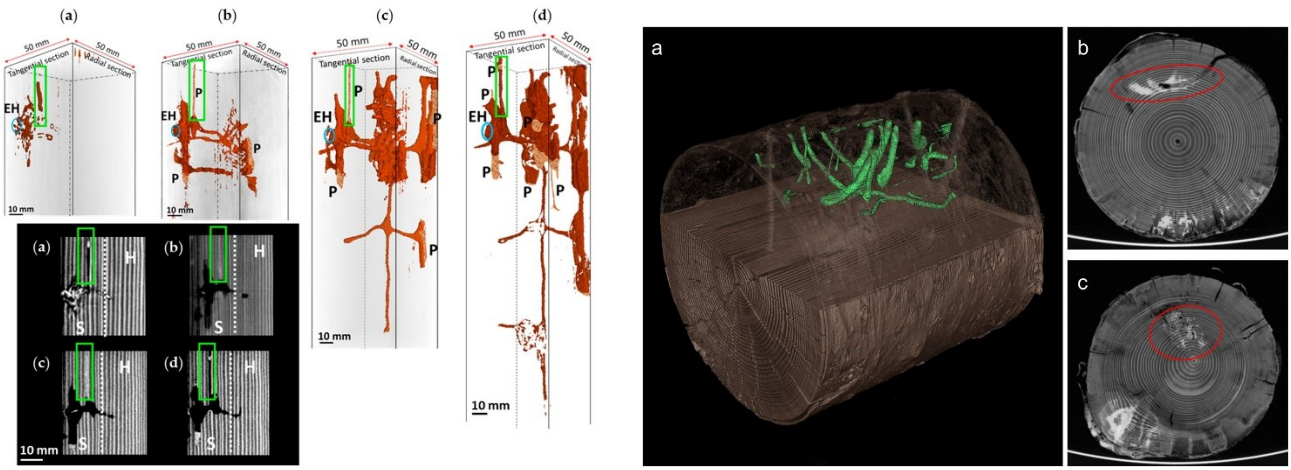

Figure 1.12. Computer Tomography has been used since early 2000s to study wood-boring insects and their galleries network. On the left, CT scans of the development of a termite nest from Himmi et al. (2016b). On the right, CT scans of various insects' galleries within deadwood, from Seibold et al. (2022), the study aimed to quantify wood decomposition using machine learning and semi-automatic image analysis.

2. OBJECTIVES

This study aims to investigate the effect of tree species on host selection and colonization success in ambrosia beetles under a simulated flooding event. More in particular, we compare how the number of entry holes (used as a proxy for host selection) and the number of successful galleries (used as proxies for colonization success) change in eight different tree species widespread in either orchard (*Malus sylvestris*, *Prunus armeniaca*, *Prunus avium* and *Pyrus pyraster*) or forest and ornamental ecosystems (*Corylus avellana*, *Carpinus betulus*, *Quercus ilex* and *Quercus robur*).

This information is very important to understand which ambrosia beetle species and which tree species can be more affected by increasing flooding events under a climate change scenario.

3. MATERIALS AND METHODS

3.1. Study site and fieldwork

A semi-field experiment was carried out in the Integrated Nature Reserve of the “Bosco Nordio”, located in the Veneto region. Bosco Nordio is a broadleaf-dominated forest, it is part of the 'Natura 2000 Network' as a Site of Community Importance (S.I.C.) and Special Protection Zone (Z.P.S.) no. IT 3250032 under EEC Directive 92/43 'Habitat' and EEC Directive 79/409 'Birds'. It represents the remains of old native forests that covered the upper part of the Adriatic coastal area (Rallo, 1992).

The forest is dominated by Holm oak (*Quercus ilex* L.) and Manna ash (*Fraxinus ornus* L.), whereas Common oak (*Quercus robur* L.), Wild linden (*Tilia cordata* Mill.), Stone pine (*Pinus pinea* L.), and White poplar (*Populus alba* L.) represent the most common secondary species.

For this project, 8 species were chosen in the orders Fagales and Rosales, selected for their common use in forestry, crop production, and ornamental use, and for the acknowledged history of ambrosia beetles targeting these tree species.

The trees from the Fagales order are Hazelnut (*Corylus avellana* L.) and European Hornbeam (*Carpinus betulus* L.), from the Betulaceae family, and Evergreen oak (*Quercus ilex* L.) and Common oak (*Quercus robur* L.) from the Fagaceae family. The trees from the Rosales order, all from the Rosaceae family, are the Apple tree (*Malus sylvestris* Mill.), Common apricot (*Prunus armeniaca* L.), Wild cherry (*Prunus avium* L.), and European wild pear (*Pyrus communis* L. subsp. *pyraster* (L.) Ehrh.).

The trees were bought from a local nursery (Vivai Guagno Ferrara), and they were all about the same size (3-5 cm diameter) and age. For each tree species, 5 individuals were bought, for a total of 40.

A pot-in-pot technique was used to simulate flood stress: the potted trees were placed inside another pot filled with water, and plastic bags were used to contain the pot and avoid spillage or draining of water. In this supersaturated environment in which the roots were immersed, the trees were stimulated to produce ethanol naturally, which attracted ambrosia beetles. The water level was periodically checked and adjusted if necessary.

Inside the Reserve, 4 glades were chosen to host 5 sites for the trees (sites 3 and 4 were in the same glade) (Fig. 3.13); each site contained 8 individuals, one for each species. Trees were randomly arranged in a straight line at 2 meters each. To secure the trees, metal wires were used to avoid bending and falling during the time of the fieldwork.

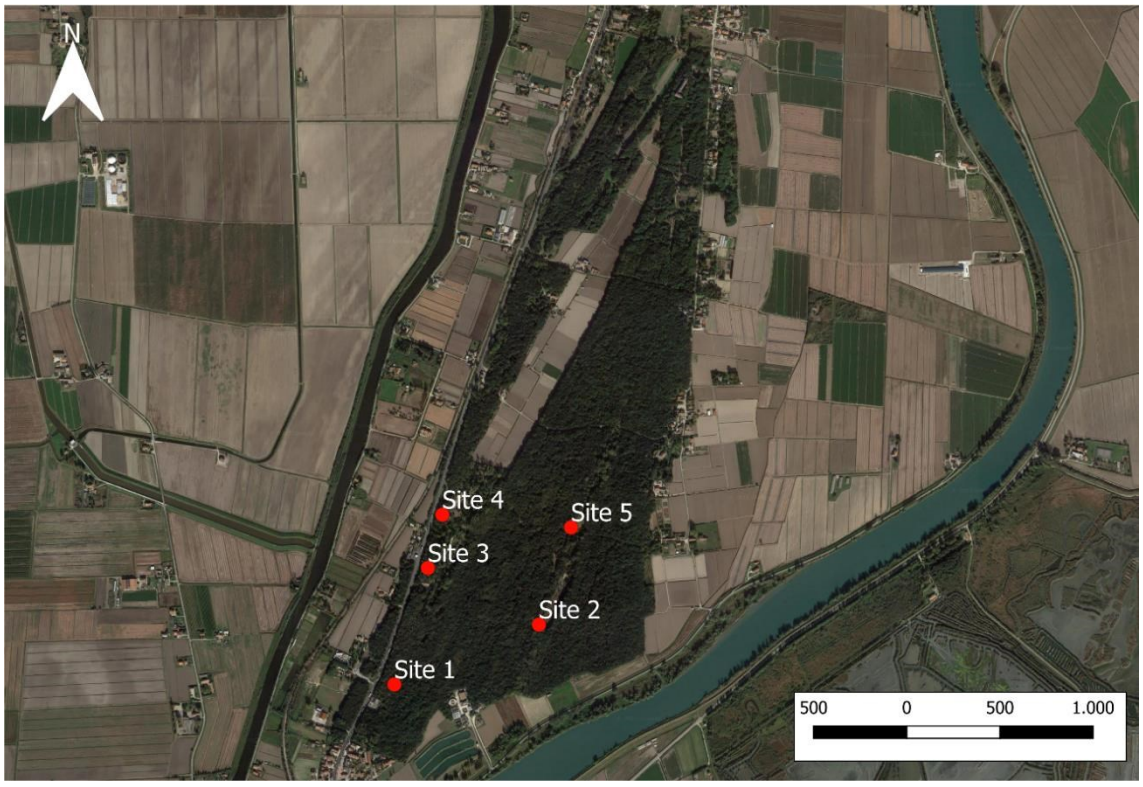

Figure 3.13. Aerial photo of Bosco Nordio. On the map, the position of the five sites chosen for this project.

The fieldwork started on the 5th of April 2022 and lasted for six weeks. After the treatments were applied to the trees, a weekly check was performed on them to register the presence of new holes dug by the insects. All the tree trunks were carefully observed and all the holes, dug by any insect, that were visible on the bark, were circled with a specific colour, associated with each week of the observation (Fig. 3.14). Week by week, every new hole was circled, so that it was possible to identify the period in which every hole was dug.

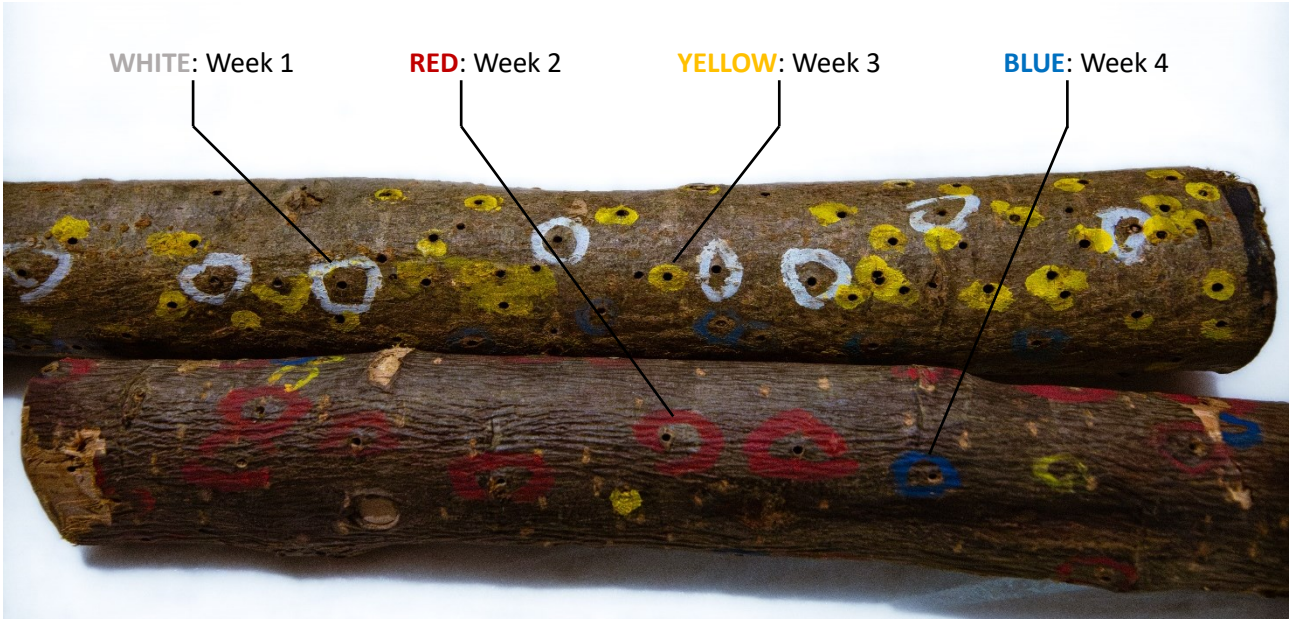

Figure 3.14. Two logs with visible and circled holes. Each colour corresponds to the week in which the hole was dug, as described on top of the image. Some holes are not circled, because they were dug on the fifth week, at the end of which all the trees were cut into logs and no more circles were drawn.

At the end of the fifth week, all the treated trees were cut into logs and brought back to the lab. For each tree, two logs were cut at different heights, so that a total of 80 logs were collected.

In the laboratory, the logs were placed in rearing chambers fitted with netting holes to allow air to circulate. Each chamber was then marked with a code to identify the logs and stored in the laboratory for five weeks. Every week, all ambrosia beetles that emerged from the logs were taken from each box and placed in previously sterilized test tubes. All the emerged ambrosia beetles present in each tube were identified into species and counted (Carloni, 2022).

The code used to identify each sample was also carved on the bark of each log and written on one of the ends where the cut was made (Fig. 3.15).

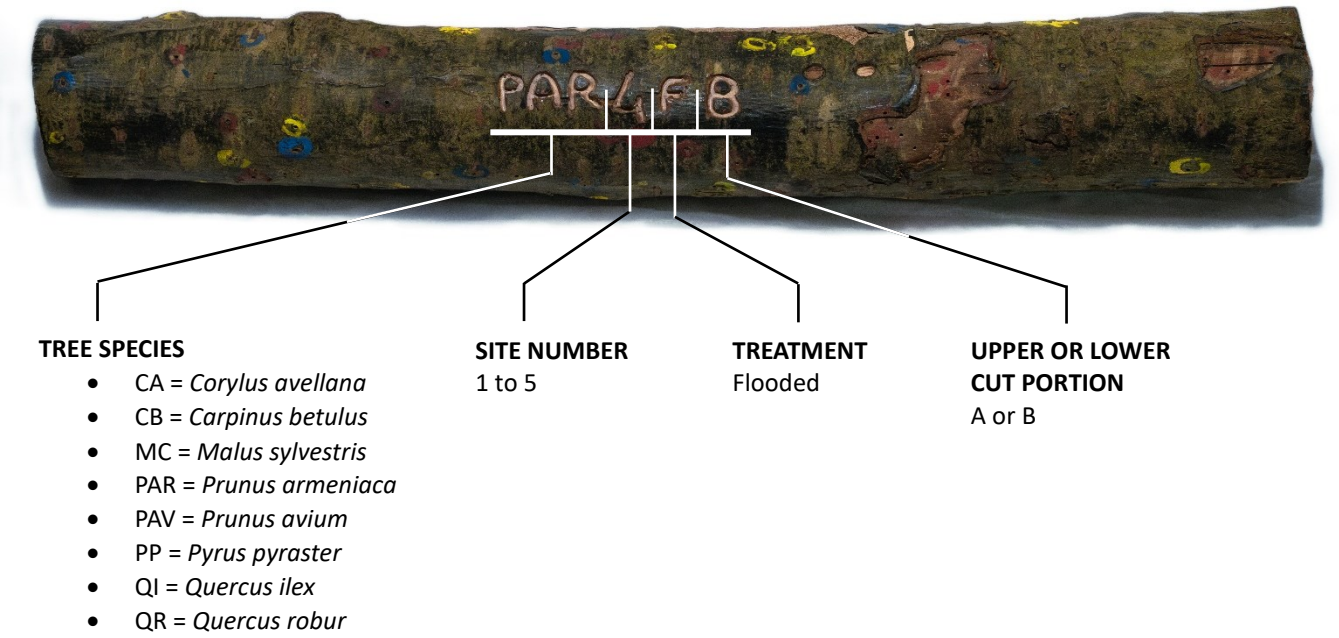

Figure 3.15. All the logs were coded by tree species, site number, treatment and cut portion, as described by the image above. The fieldwork involved other studies, that required different treatments, but for this study only the trees that underwent flooding treatment were considered.

3.2. Computer Tomography of the logs

The tomography was performed by Carl Zeiss Vision Italia S.p.A. (Fig. 3.15). All the logs underwent thermal treatment before they were sent to the labs; they were treated at 105°C for 5 days, in order to kill all the insects that remained inside the wood after the end of the experiment. This process was necessary to prevent the contamination of the tomography tools with dangerous parasites of the wood, considering that many other wooden products are analysed with the same instruments.

In this process, some of the logs lost the bark, and with it also the coloured circles around the holes that indicated in which period they were dug. To recover this data, pictures of the logs were taken before removing the bark, to allow the association with each hole to its designated colour during the analysis.

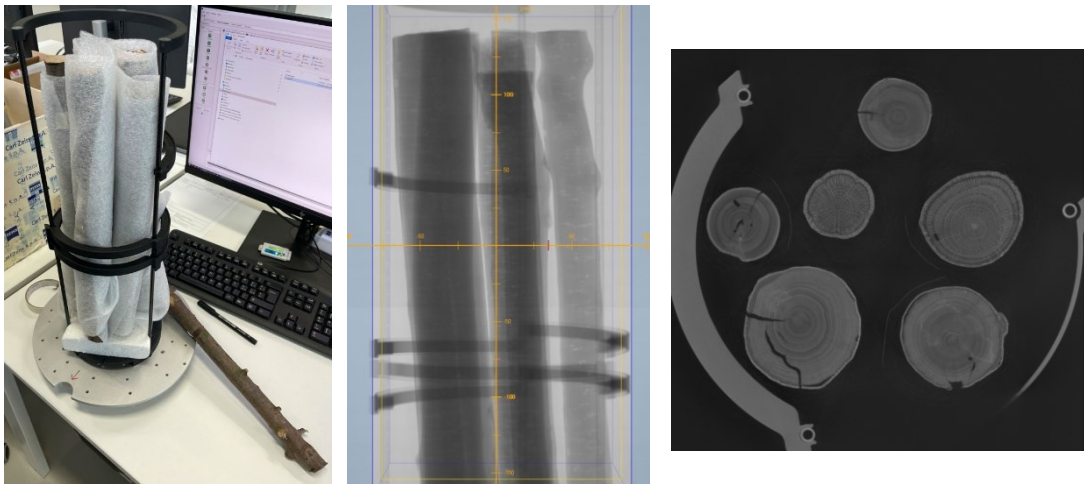

Figure 3.15. In the lab, all the logs were wrapped in a light packing material that was almost invisible to the X-rays, and they were grouped by 5 or 6, keeping them vertical and always separated.

The X-ray machinery used for the tomography was the M1500 G3, equipped with a 225 kV / 500 W X-ray tube (model Viscom XT9225D, detector Varian PS 4343 DX-I), able to produce high-resolution scans with very high accuracy. The software used to perform the X-ray scans was METROTOM OS, which is owned by ZEISS, while the scan analysis was made with VGSTUDIO MAX software.

All the scans were performed at 1.5 K resolution (1512 x 1512 px / 212 µm), excluding all the minor defects present in the log (Fig. 3.16). The tomography was able to detect all the defects and voids inside the wood, separating each of them into multiple defect masks. After that, meshes were reconstructed around every defect with different colours, to make the future sampling work easier to carry out.

After the tomography was completed, all the logs were sent back to the University of Padua with all the files associated with the digital models of each log.

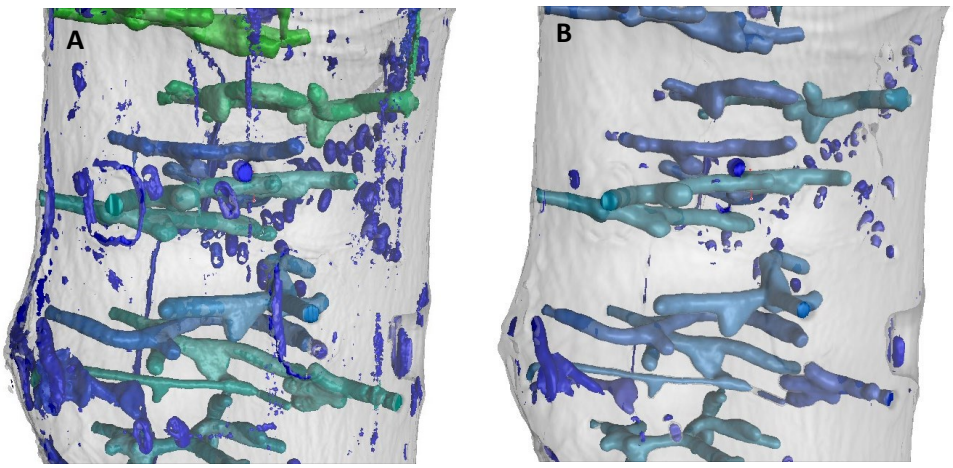

Figure 3.16. CT scans of one of the logs, performed at (**A**) 3K - 106 µm, and (**B**) 1.5K - 212 µm. The scan on the left has a better resolution, but the scan on the right has less defects, which makes it favourable for the analyses.

3.3. Observation and analysis of the digital models of the logs

All 80 logs were observed, and for every gallery dug by ambrosia beetles, much data was collected and filled into a dataset, an Excel sheet with all the information from every single gallery. The digital tools used in this process are Microsoft Excel, myVGL and Blender 3.5; myVGL was required to observe the full tomography of the log and to collect most of the data, and Blender 3.5 to reconstruct the volumes of the compromised or crossed galleries.

3.3.1. Data collection using myVGL

myVGL is a free viewer app for projects created with Volume Graphics software (VGSTUDIO and VGSTUDIO MAX format); this tool allows the user to view 3D objects in voxel, point cloud, mesh, and CAD format, the analyses and measurements performed on these objects, and the results. It is a viewer tool, which implies the impossibility of making any edit or modification to the visualized digital model.

This program was chosen for its compatibility with the files sent by ZEISS labs and for the quality and accuracy of the visualized models. It is mainly used for industrial purposes and 3D engineering, but there are several recurrences in scientific literature where this tool was applied for CT (Computer Tomography) analysis in the natural sciences field of research and, specifically, in insect ecology (Himmi et al., 2014, 2016b; Choi et al., 2017).

The interface (Fig. 3.17) is divided into 4 different panels, 3 of which are the transverse section, and the two longitudinal sections of the model, while the fourth panel is a 3D reconstruction of the full digital model of the log. On the right, a menu shows both the mesh list and different analysis tools for the volume.

Meshes are polygonal 3D models that trace and reconstruct all the defects surveyed in the digital model; thanks to their presence, it is possible to visualize every single defect and void, including the galleries dug by ambrosia beetles, and an accurate 3D reconstruction of each defect is provided.

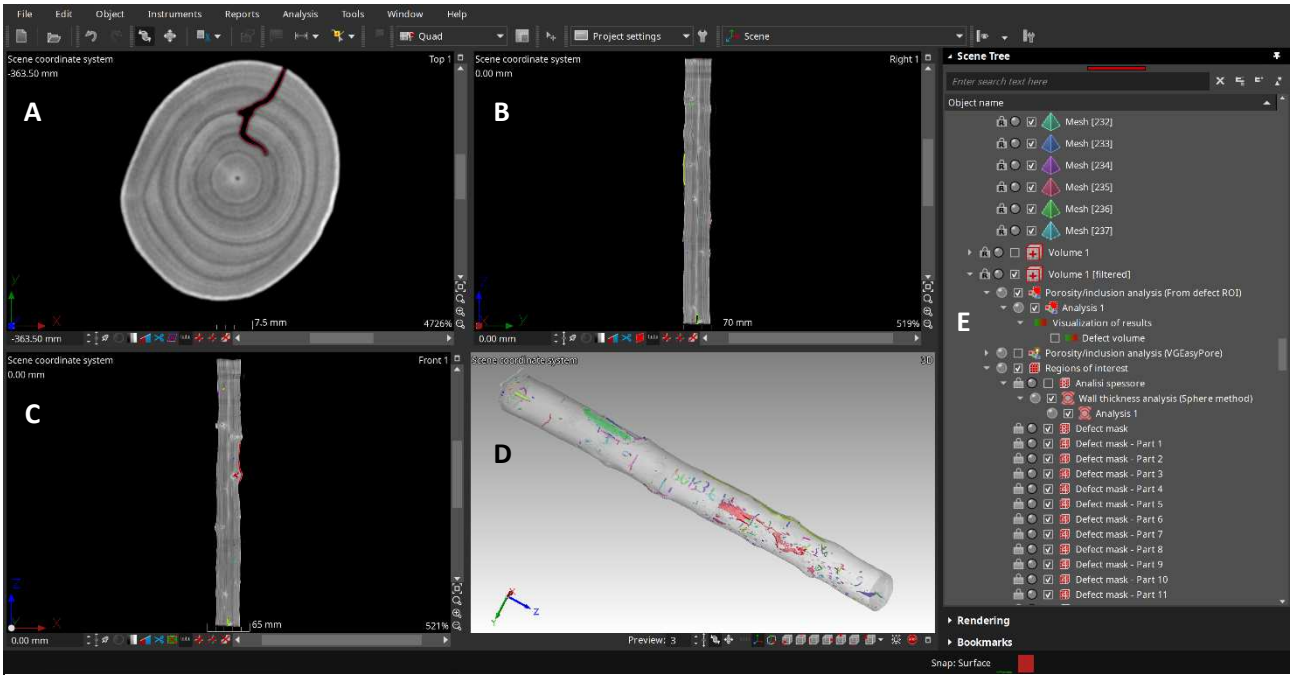

Figure 3.17. myVGL interface. (**A**) Top view. (**B**-**C**) Lateral views. (**D**) 3D model of the log. (**E**) Analysis tools, and the Defect masks list. The coloured outlines around the defects are the meshes, listed above the analysis tools.

3.3.1.1. Defect Mask and Mesh number

Every mesh is numbered and associated with a distinctive colour, allowing easy recognition of each gallery. Every mesh is associated directly with a defect mask, which is the surface occupied by the defect; mesh and defect masks share the same number (Fig 3.18). The list of the Defect masks is visible under the Regions of Interest menu, and each of them includes in their properties a volume value of that region, expressed in voxels. A voxel is a 3D pixel, used to express the volume of a digital object.

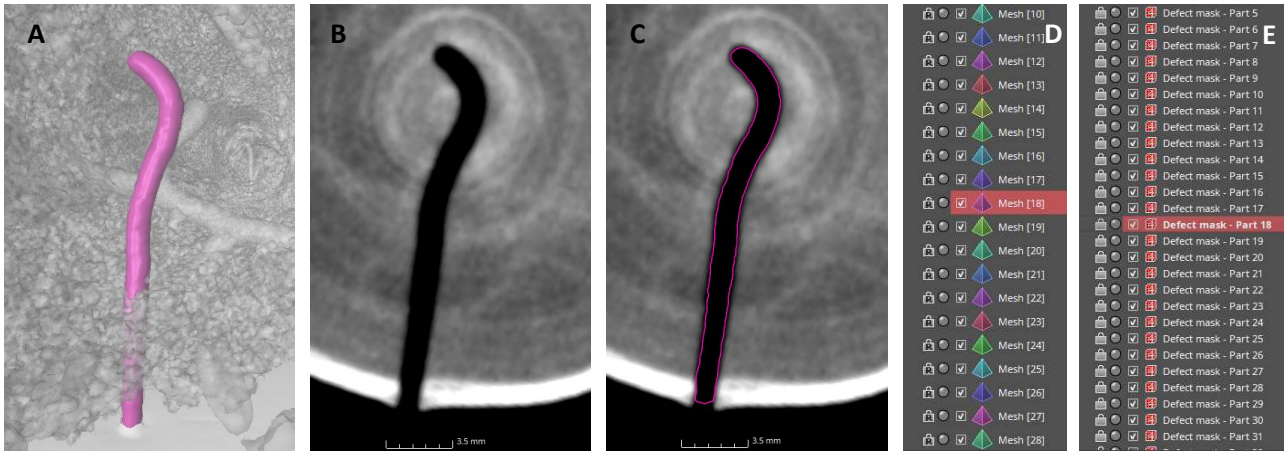

Figure 3.18. A curved gallery in PP5FA, visible in myVGL interface. (**A**) The gallery can be easily told apart from the other defects in the 3D model thanks to the colour of its mesh. (**B**) The gallery without the mesh. (**C**) The gallery with the mesh. (**D**) The Mesh list menu, where every mesh is associated with (**E**) its Defect mask.

Some galleries were not detected by the tomography (Fig. 3.19), so no mesh or defect mask was present, leaving the entry blank on the dataset. In some other cases, multiple meshes and defect masks were part of the same gallery, so only the number of the most relevant one was reported.

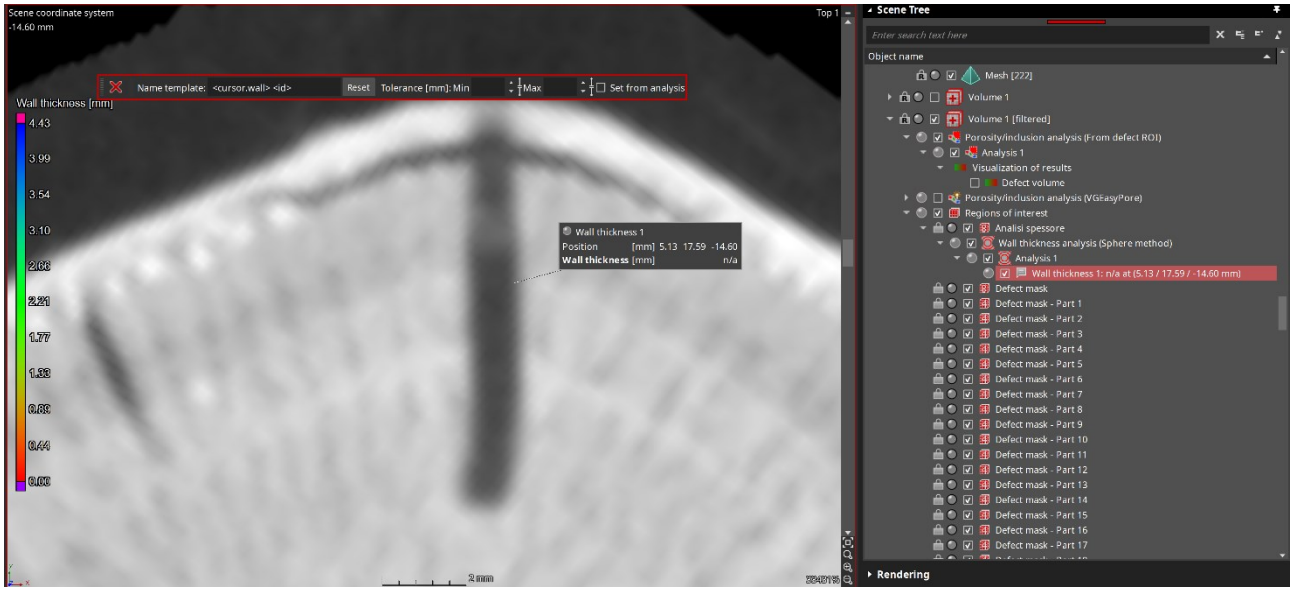

Figure 3.19. The gallery in the image has not been detected by the tomography, and no mesh or defect mask has been created. The Wall thickness analysis tool clearly shows that no data is available for this gallery.

3.3.1.2. Gallery colour

All the galleries that were visible on the bark, were circled with different colours during the fieldwork activities. When an ambrosia beetle gallery was observed in the digital model of the log, it was associated with its entrance hole that is visible on the bark. In most cases, this was easily done by just following, hole by hole, the surface of the log, or by confronting the photos of the logs taken before sending them to ZEISS labs (Fig. 3.20, 3.21).

Figure 3.20. Log QI2FA, photo taken (**A**) after the heat treatment, losing all the bark, and (**B**) before the heat treatment, with the bark still on and all the holes colours visible.

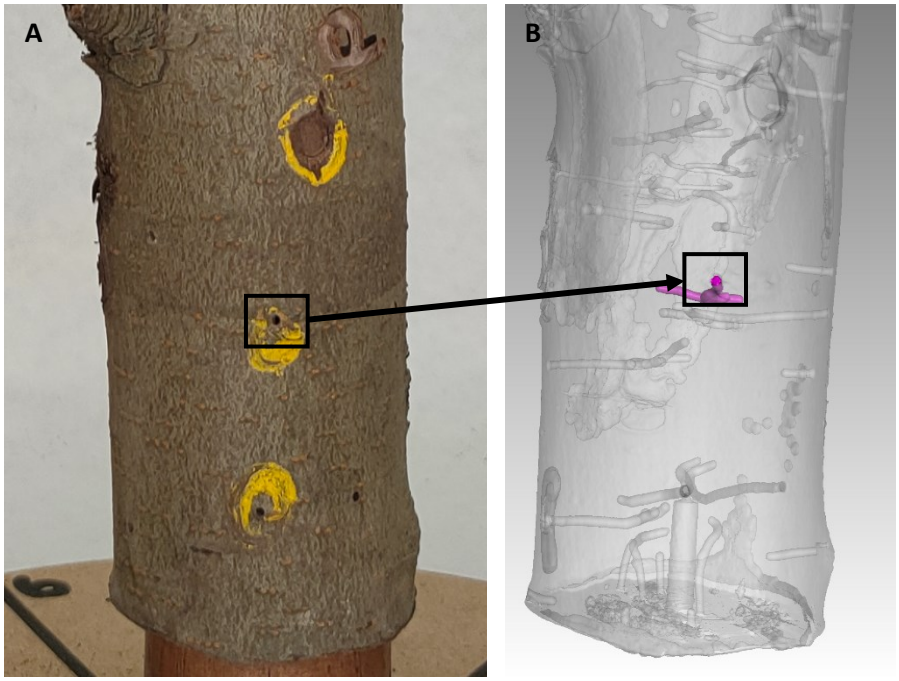

Figure 3.21. Log PP5FB, showing the association of each hole to the 3D model. (**A**) photo of the log where the entry hole is visible on the bark with its associated color, which position can be located on (**B**) the 3D model of the log, where the gallery is visible thanks to the pink mesh.

In some cases, there was no coloured circle around the hole, because some of the galleries were dug during the last week of the fieldwork before the trees were cut. In some other cases, the bark has grown over the entry hole, hiding it from sight (Fig. 3.22); these holes were classified as “hidden”, and it was not possible to determine when they were dug.

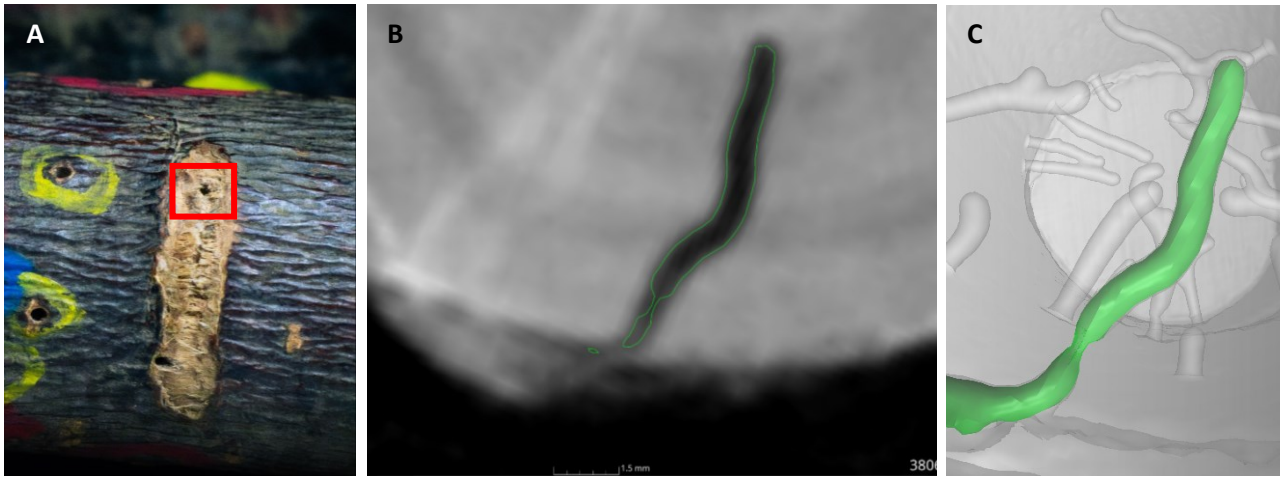

Figure 3.22. Log MC3FA, a hidden gallery. (**A**) When a gallery was observed in the tomography, but it wasn’t visible on the bark, a superficial incision was performed on the log to remove the bark and reveal the presence of an entry hole, making it visible. (**B**) in the tomography and (**C**) in the 3D model, the initial part of the gallery is visibly narrower, due to partial cicatrisation of the bark, making the hole not visible on the surface.

In some other cases, galleries originated from inside other galleries, narrower than the original (Fig. 3.23). The category “intruder” was assigned to these entries, with no colour to be assigned, as it is impossible to know when the gallery inside was dug.

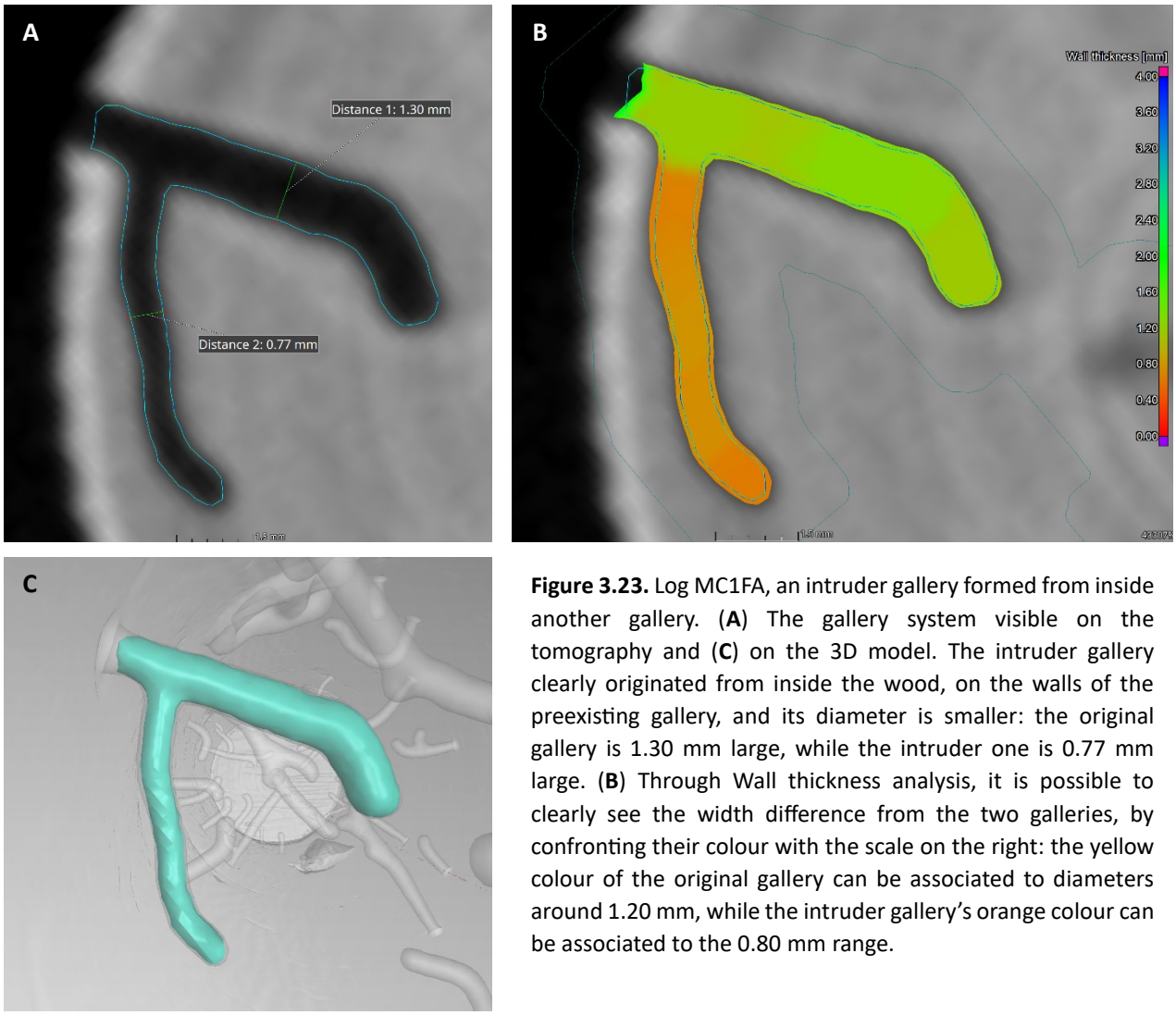

Figure 3.23. Log MC1FA, an intruder gallery formed from inside another gallery. (**A**) The gallery system visible on the tomography and (**C**) on the 3D model. The intruder gallery clearly originated from inside the wood, on the walls of the preexisting gallery, and its diameter is smaller: the original gallery is 1.30 mm large, while the intruder one is 0.77 mm large. (**B**) Through Wall thickness analysis, it is possible to clearly see the width difference from the two galleries, by confronting their colour with the scale on the right: the yellow colour of the original gallery can be associated to diameters around 1.20 mm, while the intruder gallery’s orange colour can be associated to the 0.80 mm range.

3.3.1.3. Gallery Shape and Ramifications

In most cases, the galleries were parallel to the transverse section, thus making them easy to observe and classify; when the classification was not possible from only the view of the transverse section, the 3D model of the gallery was used for observation. All the observed galleries were classified into three categories by the shape: straight (Fig. 3.24A), curved (Fig. 3.24B) or branched (Fig. 3.24C).

A value of 0 was assigned, in the ramification category of the dataset, to straight and curved galleries, indicating the presence of no ramifications, while for branched galleries, the end of each tunnel counted as a ramification, and the total number was registered into the dataset.

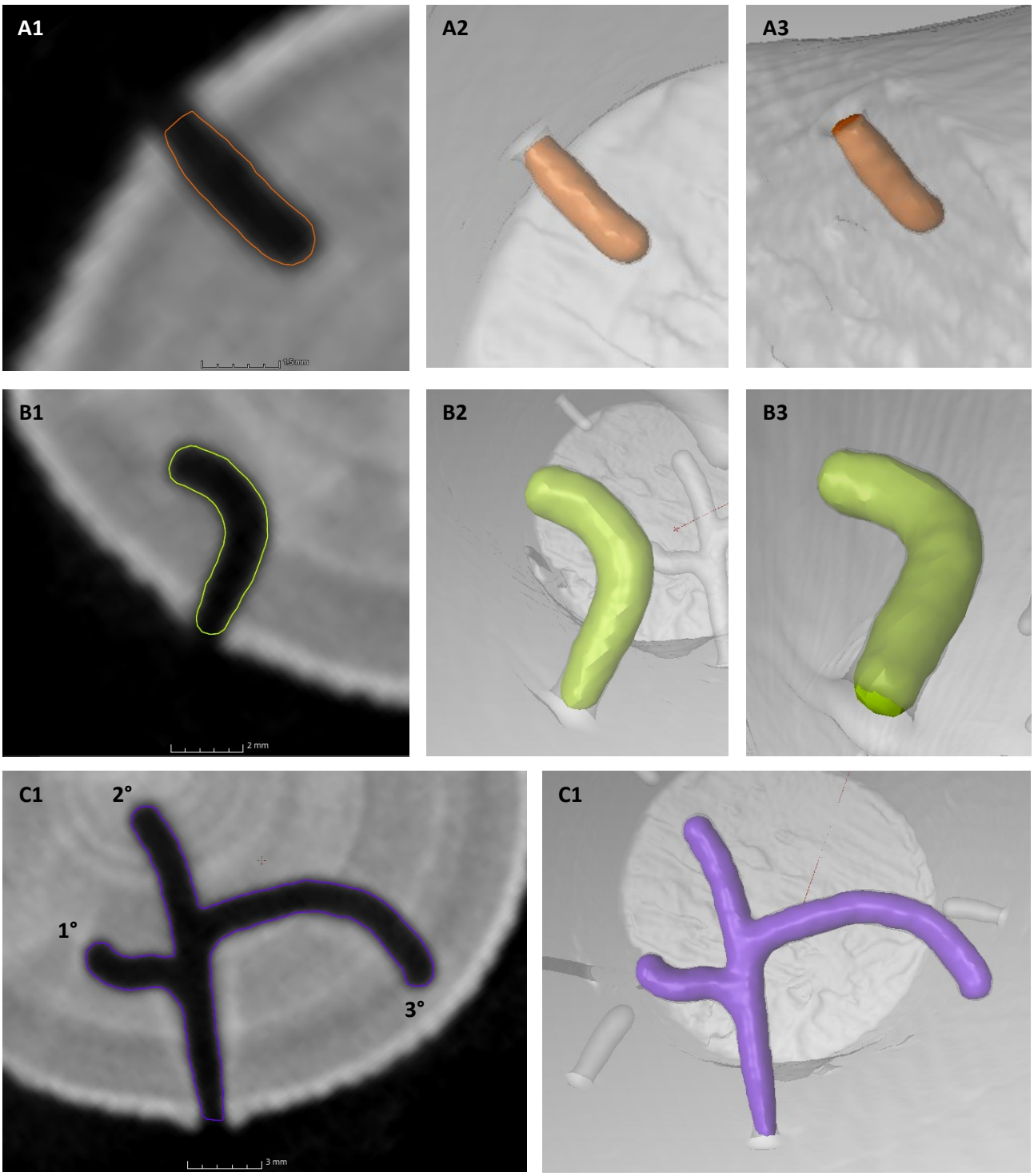

Figure 3.24. Gallery shapes classification. (**A1**-**A2**-**A3**) Straight galleries present no or lesser deviations from the general trajectory of the tunnel, that is directed towards the centre of the log. (**B1**-**B2**-**B3**) Curved galleries have a curved trajectory or present major deviations from the original direction of the tunnel. (**C1**-**C2**) Branched galleries are made of several ramifications, which can generally be clearly seen, as shown in the picture with the ramification count. In some cases, a ramification can be very short and look like bumps.

3.3.1.4. Gallery diameter

The sampling of the diameter (Fig. 3.25) required the Wall thickness analysis (Sphere method) tool under the Regions of Interest panel, which allowed the creation of an Analysis annotation on the digital model that provided a diameter value of the selected defect region. For an accurate and unbiased sampling, about 10 annotations were taken for every gallery, each at an equal distance from the other, avoiding regions where the reconstruction of the gallery was visibly compromised. Some galleries were very short and required fewer annotations, while others, especially branched galleries, required more annotations, distributed on the different branches.

The total diameter was calculated as the mathematical average of the annotations. In some cases, the whole gallery needed a total reconstruction, so an approximate diameter was taken at different levels with the Caliper tool, directly on the transverse section view.

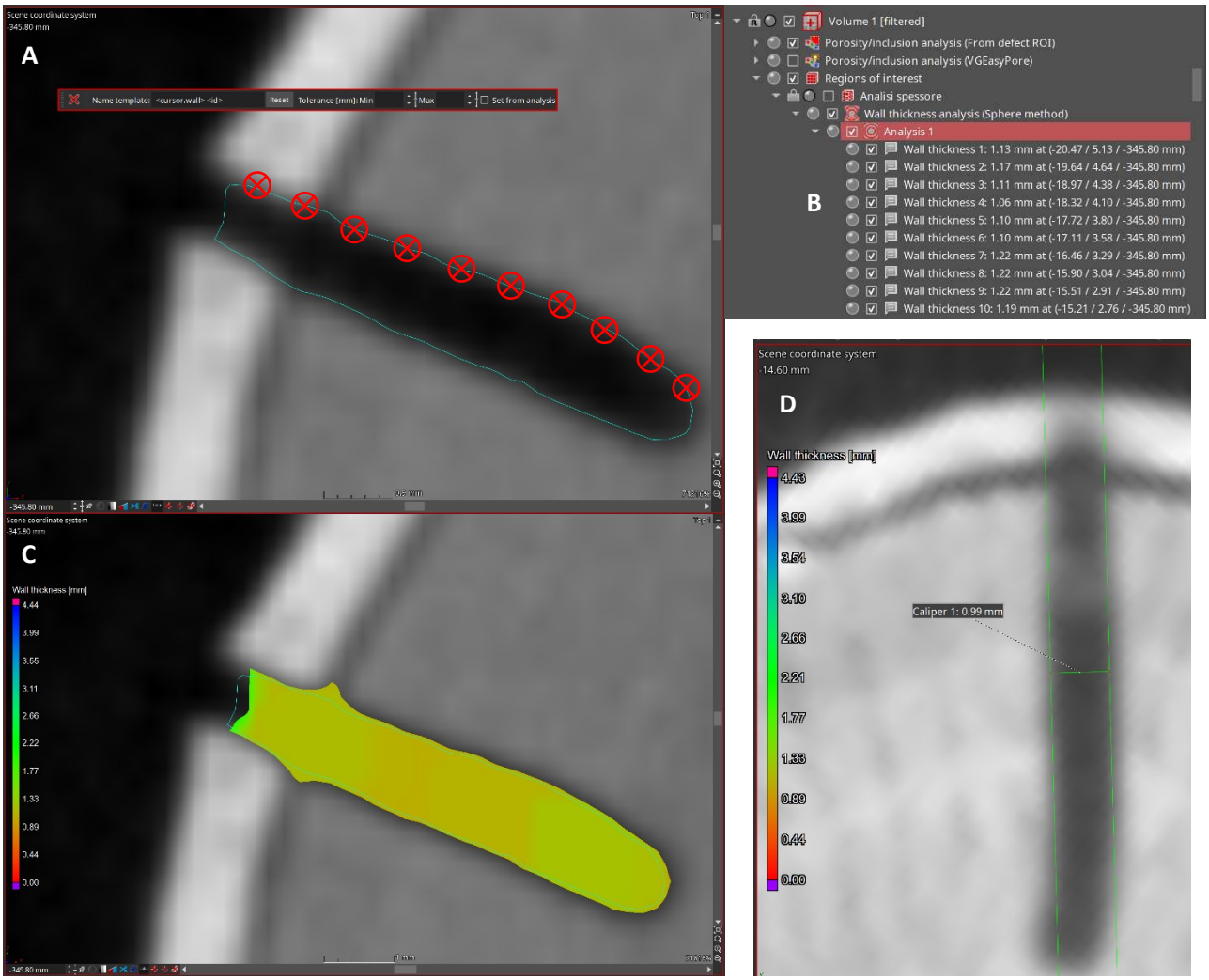

Figure 3.25. Diameter measuring. (**A**) The sampling is done by choosing 10 points or more on the gallery edge that are equally distant (red marks on the image), then the average is calculated with (**B**) the annotations. (**C**) Wall thickness analysis, visible with colours. (**D**) Diameter reconstruction using the Caliper tool, to sample the diameter correctly.

3.3.1.5. Gallery volume

Under the Data from Porosity/inclusion analysis (From defect ROI) panel, the Analysis tool allows the creation of annotations for the volume of the selected defect (Fig. 3.26); moreover, it gives access to a Defects table where all the defects are listed, providing important information for each of them, among which the volume is the most relevant.

When a gallery was observed, the Porosity/inclusion analysis tool was used to sample the volume. This value was present in the Defects table of the Porosity/Inclusion analysis panel, so in this way, it was possible to associate each defect present in the table with a specific defect mask and mesh.

The line of the interested defect was reported in the dataset; in this way, the volume and all the other information related to the gallery were provided.

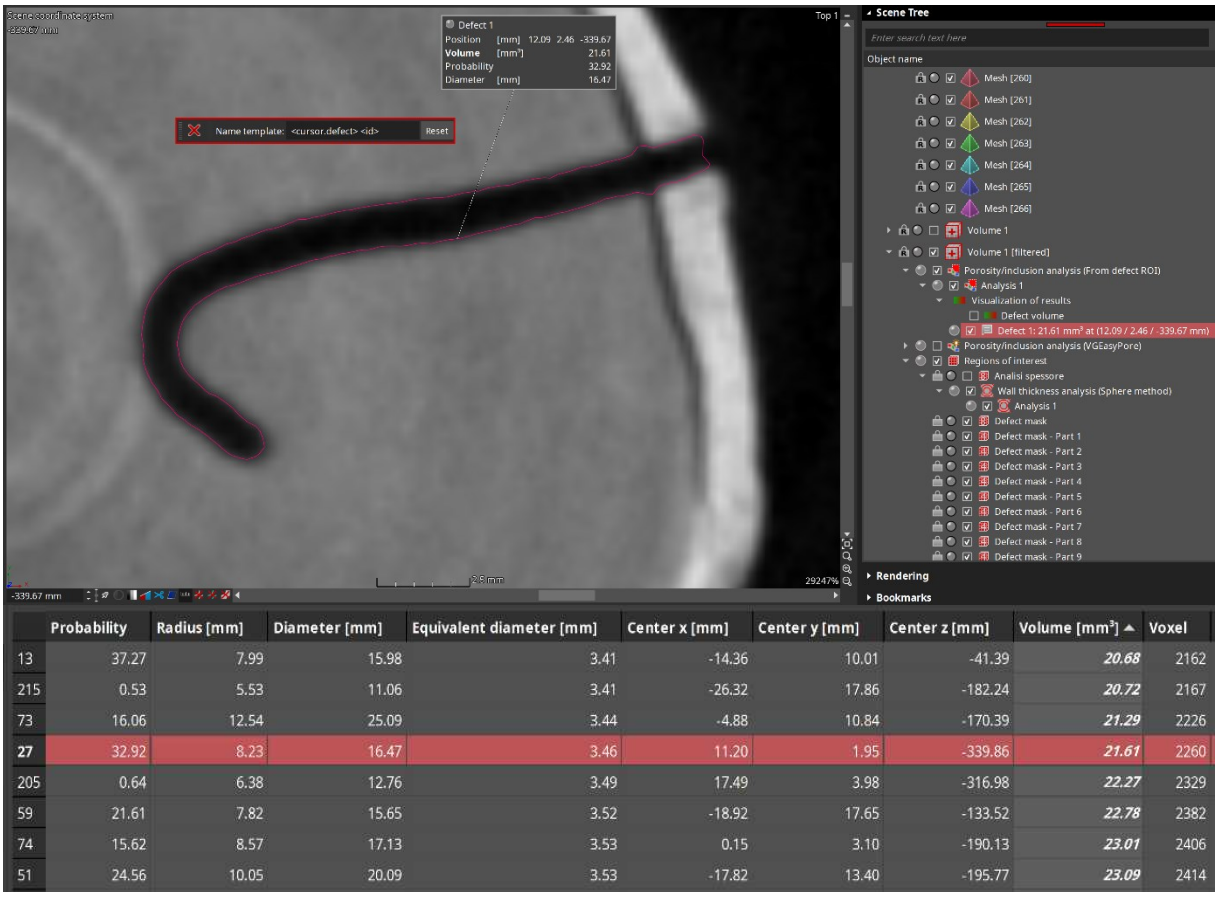

	Probability	Radius [mm]	Diameter [mm]	Equivalent diameter [mm]	Center x [mm]	Center y [mm]	Center z [mm]	Volume [mm³]	Voxel
13	37.27	7.99	15.98	3.41	-14.36	10.01	-41.39	*20.68*	2162
215	0.53	5.53	11.06	3.41	-26.32	17.86	-182.24	*20.72*	2167
73	16.06	12.54	25.09	3.44	-4.88	10.84	-170.39	*21.29*	2226
27	32.92	8.23	16.47	3.46	11.20	1.95	-339.86	*21.61*	2260
205	0.64	6.38	12.76	3.49	17.49	3.98	-316.98	*22.27*	2329
59	21.61	7.82	15.65	3.52	-18.92	17.65	-133.52	*22.78*	2382
74	15.62	8.57	17.13	3.53	0.15	3.10	-190.13	*23.01*	2406
51	24.56	10.05	20.09	3.53	-17.82	13.40	-195.77	*23.09*	2414

Figure 3.26. Volume sampling. Using the Porosity/inclusion analysis (From defect to ROI) tool, it is possible to sample the volume of a gallery, which value can be seen on a small tab connected to the gallery and as an annotation on the menu, under the Analysis tool. In the Porosity/inclusion analysis properties, the Defect table, visible on the bottom, can be accessed. Inside of it, the list of all the defects is present and they can be sorted by volume.

3.3.2. Species recognition

Each ambrosia beetle species digs very narrow entry holes and galleries that can be directly associated with their sizes, making it possible to recognize the insect species that dug each gallery by association with a given diameter range.

From previous studies on these logs, emerging adults have been counted and classified by species (Carloni, 2022), and four insect species were found: *Xyleborinus saxesenii*, *Xylosandrus germanus*, *Xylosandrus crassiusculus* and *Anisandrus dispar*. A diameter range has been established for each insect species, considering previous research and scientific literature (Rassati et al., 2020; Ranger et al., 2016) about the size of the entry holes of each insect species (Fig. 3.27).

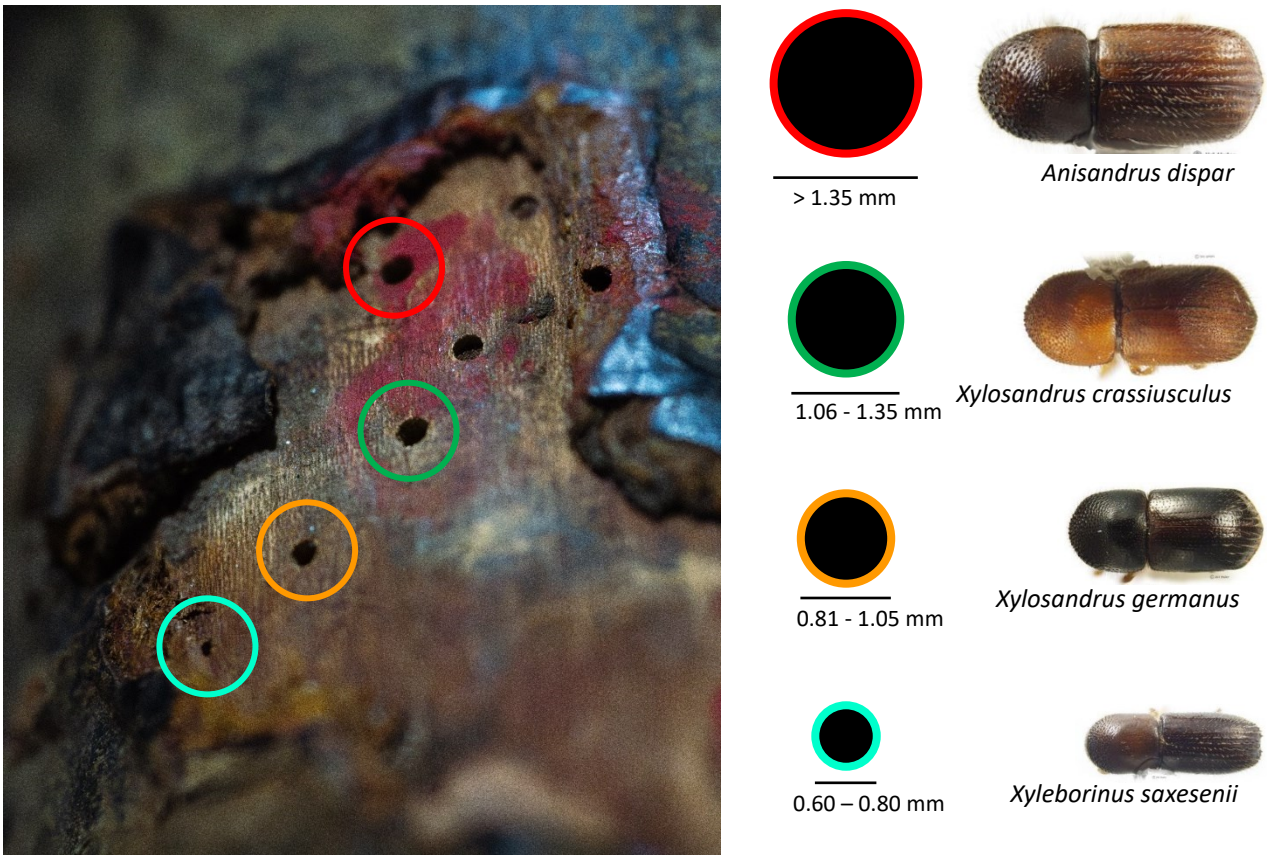

Figure 3.27. Each insect species was assigned to a specific diameter range. On the picture, a portion of wood where the four circled entry holes were assigned to a different insect species each. *A. dispar* digs the largest holes, bigger than 1.35 mm. *X. crassiusculus* digs holes that are 1.06 to 1.35 mm large. *X. germanus* digs holes that are 0.81 to 1.05 mm large. Finally, *X. saxesenii* digs the narrowest holes, which are 0.60 to 0.80 mm large.

3.3.3. Volume reconstruction using Blender 3.5

In many cases, the defects detected by the tomography were affected by some form of damage that represented important obstacles for the sampling and measurement of the galleries (Fig. 3.28). In some cases, the gallery was divided into two or more different meshes or some portions of the gallery were not detected. For these galleries, a simple sum across all the volumes that are part of the gallery was made, while the volume of the missing portions was reconstructed using the cylindric volume formula, including the length of the portion (sampled with the Distance tool) and the mean diameter of the gallery.

$$Volume = \left(\frac{d}{2}\right)^2 \cdot \pi \cdot l$$

d = diameter of the gallery

l = length of the gallery (measured with Distance tool)

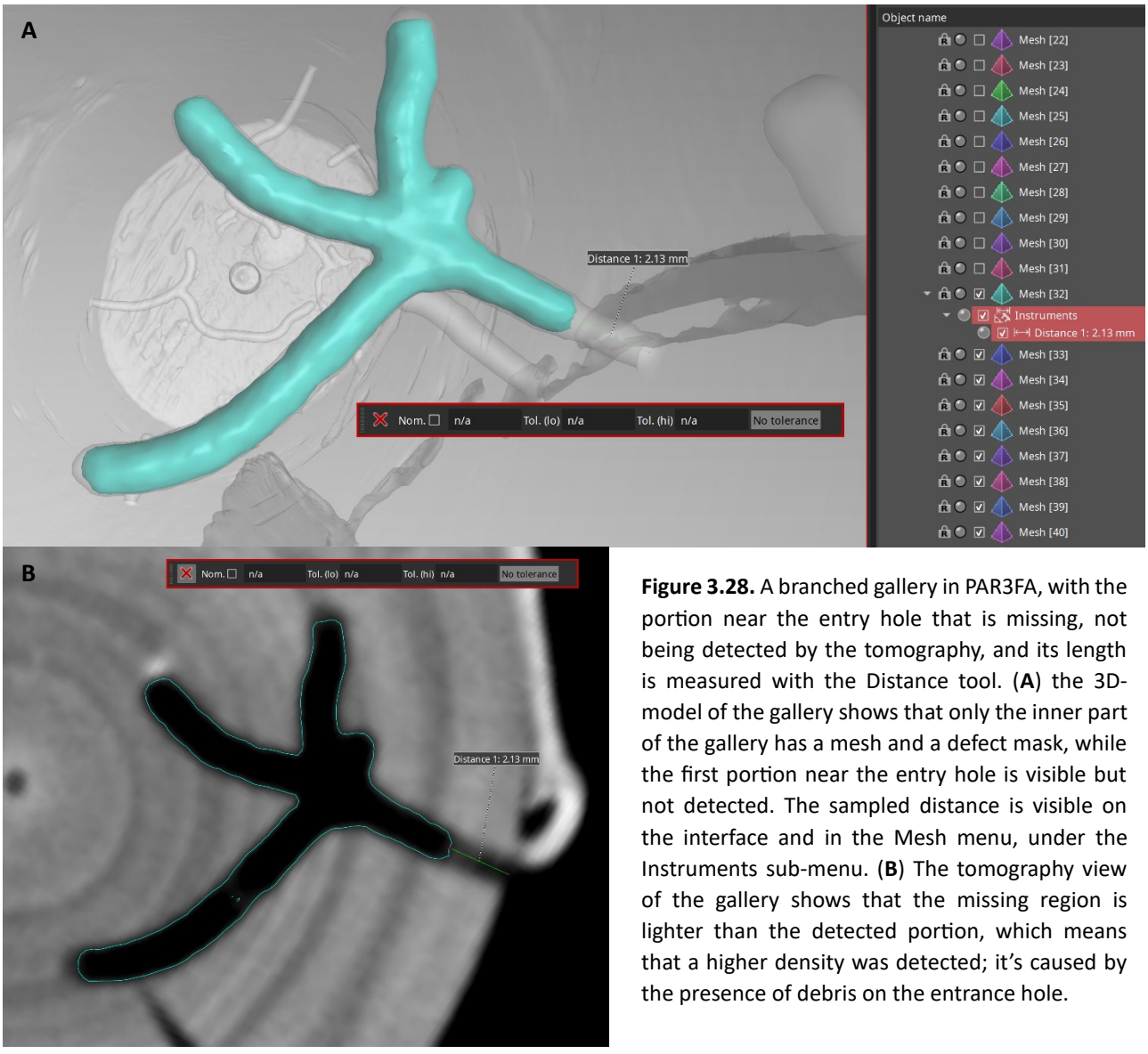

Figure 3.28. A branched gallery in PAR3FA, with the portion near the entry hole that is missing, not being detected by the tomography, and its length is measured with the Distance tool. (**A**) the 3D-model of the gallery shows that only the inner part of the gallery has a mesh and a defect mask, while the first portion near the entry hole is visible but not detected. The sampled distance is visible on the interface and in the Mesh menu, under the Instruments sub-menu. (**B**) The tomography view of the gallery shows that the missing region is lighter than the detected portion, which means that a higher density was detected; it's caused by the presence of debris on the entrance hole.

There were also galleries fused into a single defect, as they were intersecting or touching each other. In some other cases, there was a bigger defect, such as a wood crack or a void space between the bark and the sapwood, that grouped into a single defect all the galleries that were touching it.

In all these cases, the only data that was compromised was the volume, which needed reconstruction. To do so, a different software was used: Blender 3.5. This is a free and open-source software that is widely used in 3D modelling, supported by major hardware sellers and producers such as AMD, Apple, Intel, and NVIDIA.

Blender 3.5 is able to read the STL file format, which is used for the meshes, and is provided with an add-on for dimensional and volumetric measuring of the 3D models, called 3D-Print Toolbox. In this way, it is possible to import any gallery's mesh inside the program to sculpt and model it to fix all the ruined sections and to separate the merged defects and galleries.

Whenever a gallery needed some form of reconstruction, the values in the Defect table of the Porosity/inclusion analysis panel in myVGL were ignored, and the reconstructed value was reported in the dataset under its specific column.

3.3.3.1. Cleaning merged defects

In many cases, void regions such as wood cracks, spaces between the bark and the sapwood, or even generated by the surface features of the bark, are connected to a gallery, thus merging the defect with the galleries that are touching or crossing it (Fig. 3.29). If the defect is big enough to significantly influence the volume, a reconstruction is required.

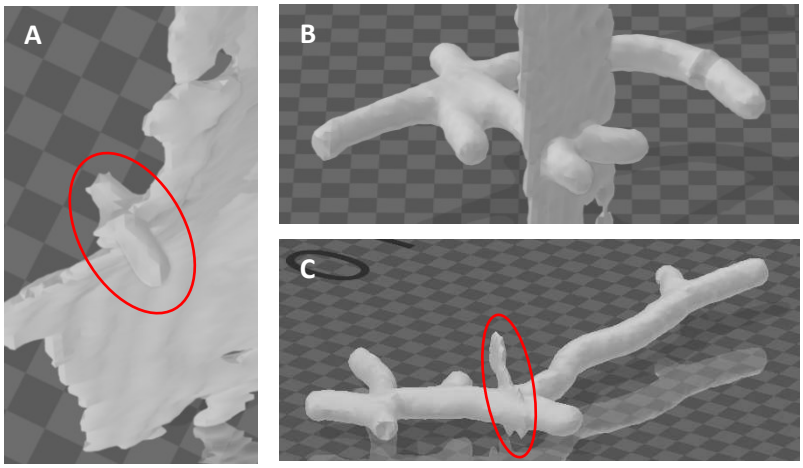

Figure 3.29. (**A**) A straight gallery, visible inside the red circle, was merged with a wide flat defect, originated from the separation of the bark from the inner wood, which left a void region. (**B**) A branched gallery that crossed a flat defect, originated from a wood crack. (**C**) A branched gallery had another defect merged together, highlighted by the red circle, originated from a void region inside the wood.

In Blender, the meshes were imported and their total volume was sampled by the 3D-Print toolbox. After that, the mesh was edited, deleting the portions of the unwanted defect, and closing the open gaps using the Inset Faces tool (Fig. 3.30). Once cleaned, the mesh volume was measured again.

The final volume obtained in this way is not accurate: meshes are reconstructed by tracing the defects, but the associated Defect mask in myVGL provides more reliable data (Fig. 3.31). To get the most accurate volume from the reconstruction, the original volume of the gallery sampled with the Porosity/inclusion Analysis tool in myVGL was divided by the original volume detected in Blender and then multiplied by the final volume sampled after the reconstruction in Blender.

$$Reconstructed\ volume = \frac{V_i\ myVGL}{V_i\ Blender} \cdot V_f\ Blender$$

Vi myVGL = Original volume sampled in myVGL

Vi Blender = Original volume sampled in Blender

Vf Blender = Volume after reconstruction, sampled in Blender

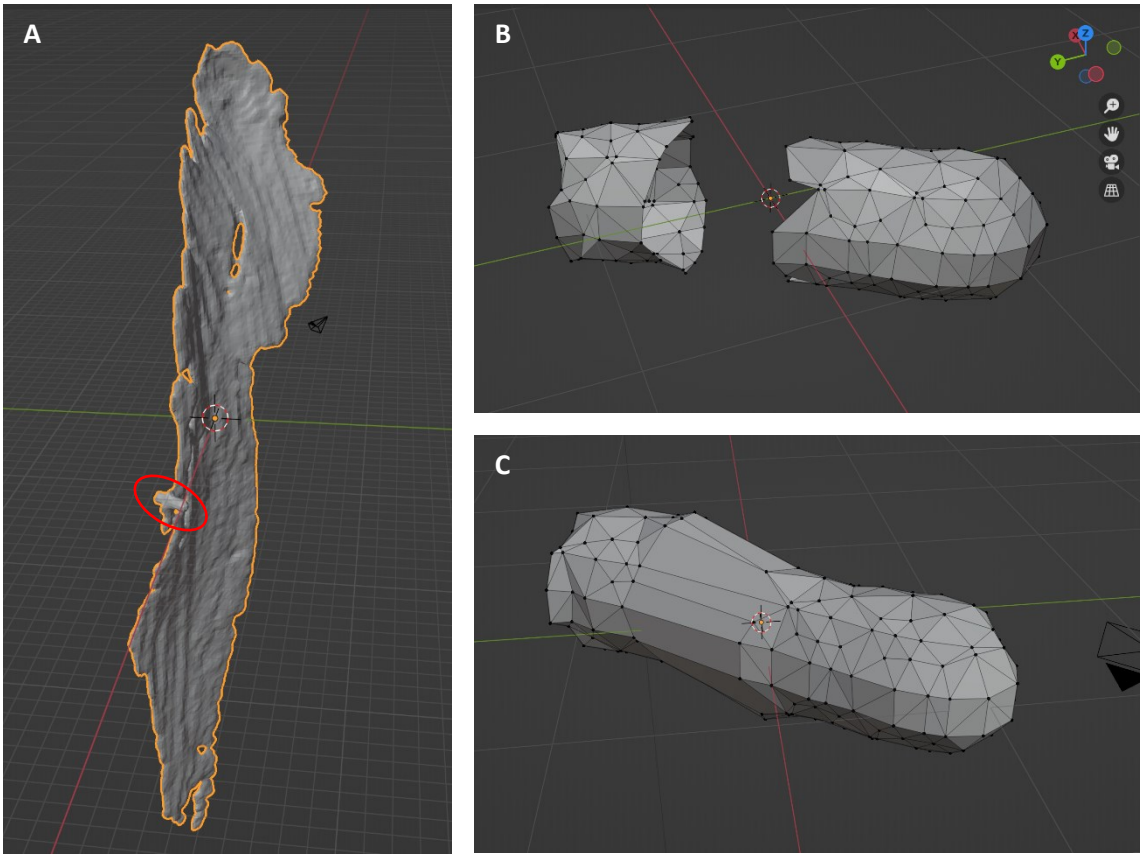

Figure 3.30. The mesh visualized in Blender 3.5 of a straight gallery merged with a defect originated from a wide space between the bark and the wood, needs reconstruction. (**A**) The gallery, highlighted by the red circle, must be isolated from the rest of the defect, that is erased. (**B**) After the cleaning, the gallery needs to be reconstructed. (**C**) The reconstructed volume can be sampled for its volume.

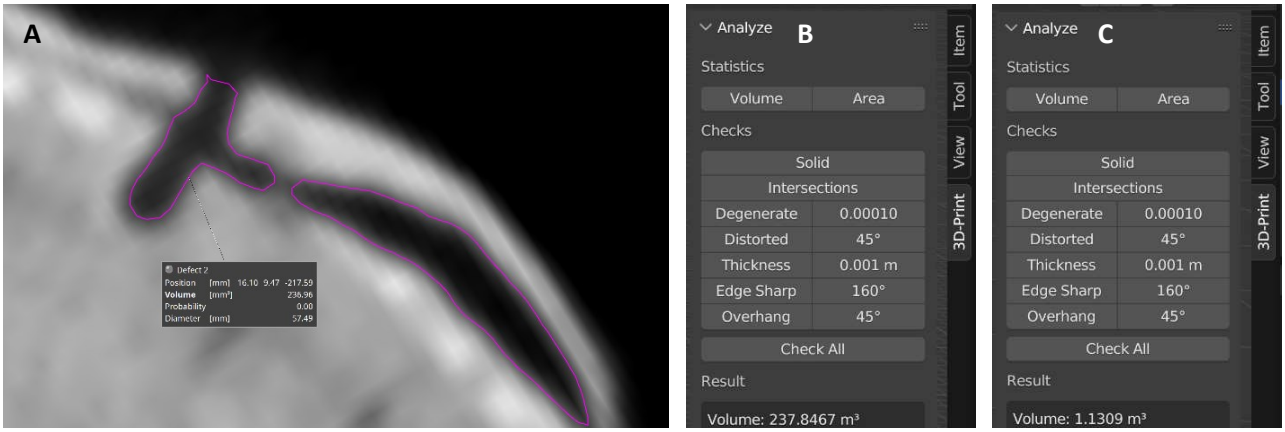

Figure 3.31. (**A**) The same mesh of Fig. 30 visualized in myVGL, the volume can be sampled with the Porosity/inclusion analysis tool. (**B**-**C**) The 3D-print toolboxes of the mesh in Fig. 30, visualized in Blender 3.5, before reconstructing the volume and after.

In some cases, multiple galleries were crossing or touching the same defect, merging them together (Fig. 3.32). In the cleaning procedure, each gallery was separated into individual meshes and the volume was reconstructed individually for each of them. In the dataset, these galleries were listed individually and the entry “NO” was given under the Crossed Galleries column. All these galleries were reported with the same mesh and defect mask number.

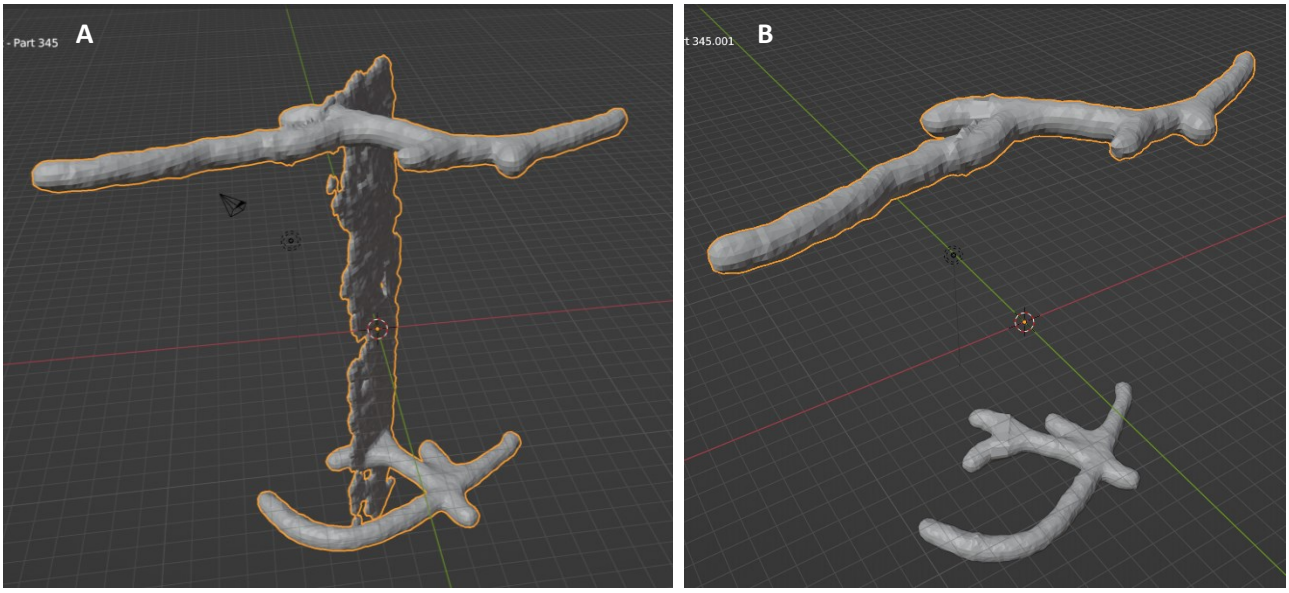

Figure 3.32. (**A**) Two branched galleries, both crossing the same wood crack, need to be separated and cleaned. (**B**) After the cleaning of the wood crack defect, and the separation, the two galleries can be sampled individually for the volume.

3.3.3.2. Separating crossed galleries

When multiple galleries intersect or touch each other, they merge into a single mesh and need to be separated to reconstruct the volume correctly (Fig. 3.33). The mesh is imported in Blender and its total volume must be written down, it is edited to separate the galleries and for each of them, the final volume must be obtained.

Both the volume of the separated galleries obtained in Blender with the 3D-Print toolbox must be divided individually by the original volume of the mesh. This ratio represents the percentage of volume that each gallery occupies in the defect. This percentage is filled in the Sub Gallery Percentage column of the dataset, together with the entry "YES" under the column Crossed Galleries. The crossed galleries are listed individually in the dataset, each with their volume percentage and the same mesh and defect mask number associated.

$$Gallery\ volume\ \% = \frac{V_g}{V_i} \cdot 100$$

Vg = Volume of the single gallery

Vi = Volume of the merged galleries

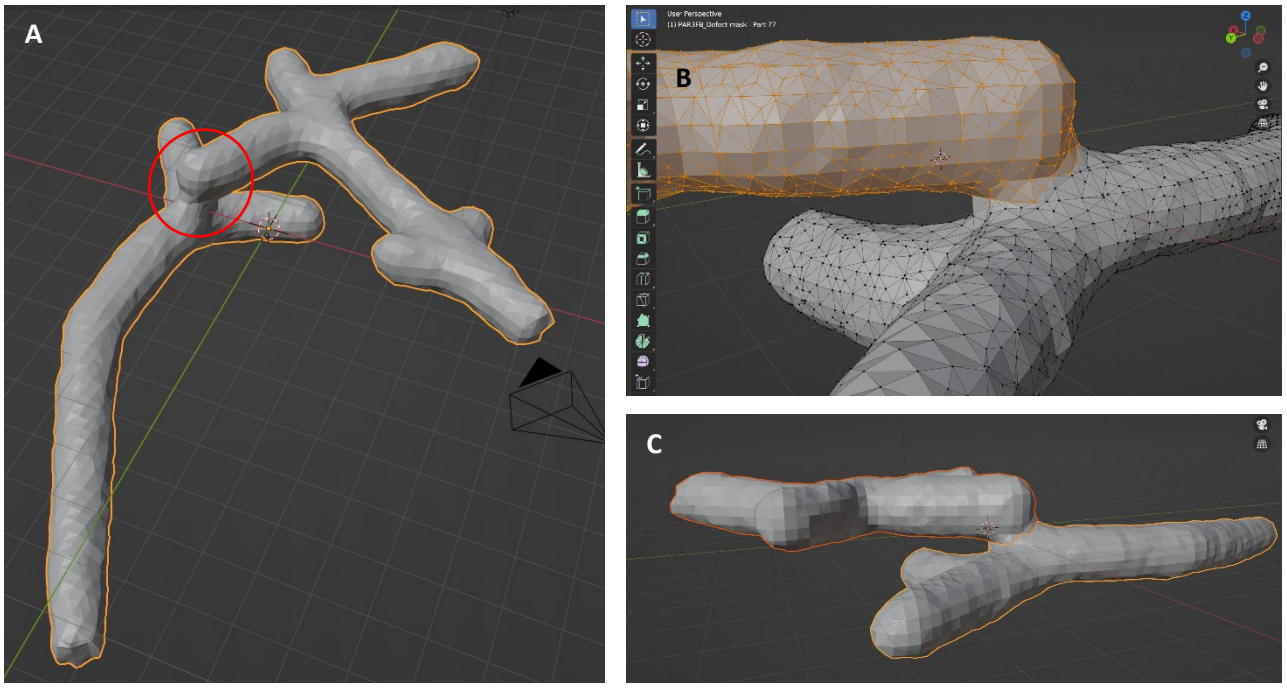

Figure 3.33. Two branched galleries visualized in Blender 3.5 are crossing each other. (**A**) The galleries are touching in the point where the red circle is drawn. (**B**) To separate them, one of the two galleries is selected, and, at the junction point, the selection is made to include each polygonal face that is considered part of the gallery. (**C**) After the separation, each gallery is sampled individually, and the volume is divided by the original, to get the gallery volume percentage.

To obtain the reconstructed volume, the Porosity/inclusion analysis tool in myVGL was used to sample the volume, which was multiplied by the gallery volume percentage, and the result was filled in the Reconstructed Volume column of the dataset.

$$Reconstructed\ volume = V_i\ myVGL\ \cdot g\%$$

Vi myVGL = Original volume, sampled with myVGL

g% = Gallery volume percentage

This process was also applied to the galleries that originated from inside other galleries, separating each of them (Fig. 3.34). The galleries originated from inside others were given the "INTRUDER" entry under the Crossed Galleries column.

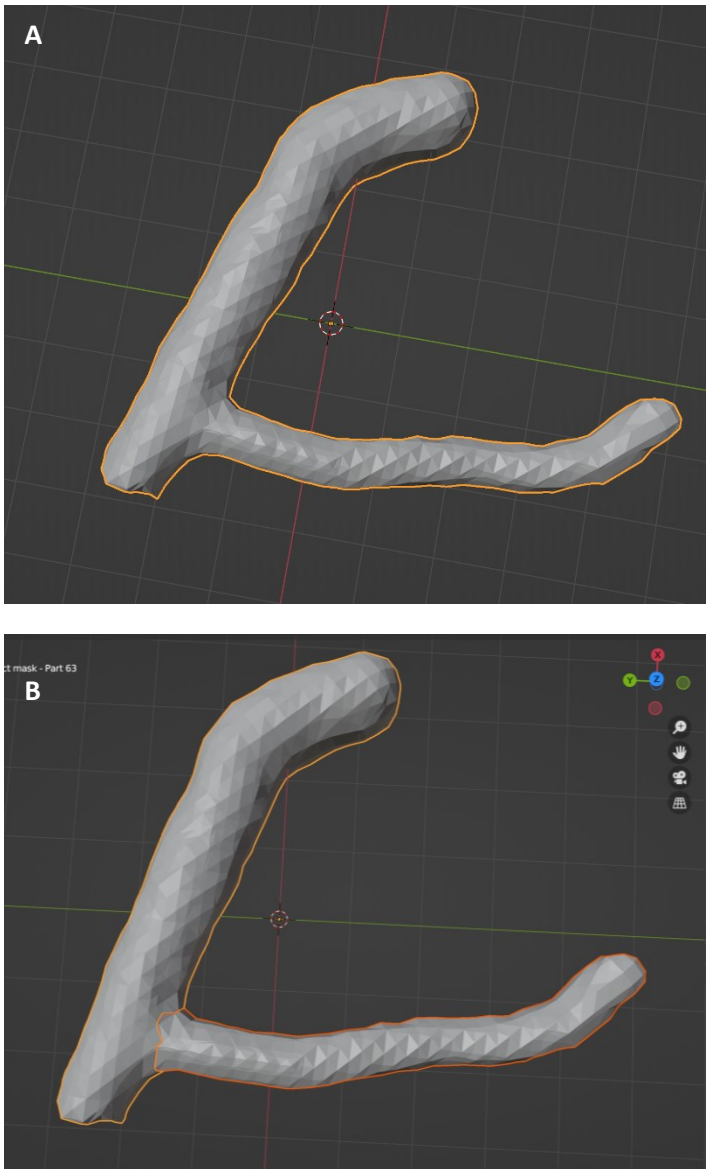

Figure 3.34. The same gallery system from Fig. 23, made of a curved gallery and another narrower one, originated from inside it, visualized in Blender 3.5. (**A**) The two galleries are merged together and need to be separated, in the same way performed in previous cases. (**B**) After the separation, which is visible thanks to the different colours of the edges of the 3D model, the two galleries are sampled individually and each gallery volume percentage is calculated, following the same steps for crossed galleries.

3.3.3.3. Reconstruction by joining split galleries

Some rare cases occurred where a wood crack or a void in the bark divided the gallery, splitting it in two (Fig. 3.35). In these cases, the reconstruction was carried out following the ordinary procedures, but after the unwanted defect portions were cleaned, the gallery was manually reconstructed, by joining the separated parts of the galleries and merging them back together.

When the splitting occurred along the whole length of the gallery, for a wood crack that crossed a straight gallery, the diameter of the gallery was compromised, and it required a different sampling procedure.

The diameter was sampled normally and also the width of the wood crack was sampled with the Wall thickness analysis tool at the two ends of the gallery, moving the Top view to a point where it was possible to sample it. In this way, it was possible to calculate the average width of the crack across the gallery, and then it was subtracted from the diameter previously sampled.

$$Split\ gallery\ diameter = d_i - d_c$$

di = Diameter sampled normally

dc = average width of the wood crack

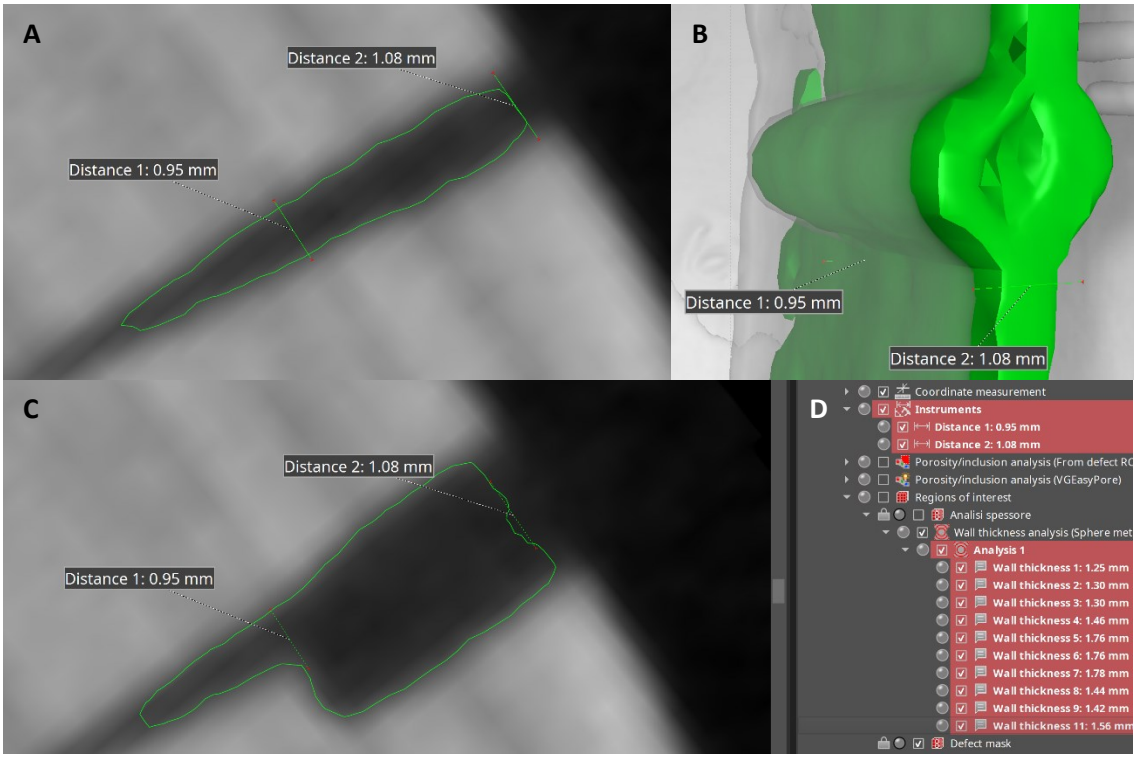

Figure 3.35. A straight gallery in PAR1FA, split in two by a wood crack. (**A**) The diameter of the crack is measured at two points aligned with the entry hole and the end of the gallery. (**B**) The two points where the crack width is sampled are right below the wood gallery. (**C**) The diameter of the gallery is sampled normally, but the width of the wood crack must be subtracted. It is visible that the two width measurements for the wood crack correspond to the entry hole and to the end of the gallery. (**D**) All the values are visible in the menu on the right.

3.4. Statistical analysis

All the analyses were carried out in R software (R Core Team, 2021). To evaluate the effect of the plant species on the number of entry holes, for each of the three insect species a generalized linear model (GLM) with a negative binomial distribution (log link-function) was built and validated. The response variable was the number of entry holes counted per log. The categorical explanatory variable was the plant species (eight levels). To evaluate the effect of the plant species on the colonization success, for each of the three insect species a linear model (LM) with a Gaussian distribution was built and validated. The response variable was the percentage of branched galleries on the total number of galleries. The categorical explanatory variable was the plant species (eight levels). Pairwise multiple comparisons were run using post-hoc tests with Tukey correction of p-values. All the analyses were carried out in R software (R Core Team, 2021).

4. RESULTS

4.1. General observations

A total of 2318 galleries over 80 logs collected from 40 trees of 8 different species, were observed and analyzed for this thesis. Among them, both branched, straight, and curved galleries were observed in a significative number for 3 out of 4 surveyed ambrosia beetle species: *Xylosandrus crassiusculus*, *Xylosandrus germanus* and *Xyleborinus saxesenii*. Very few *Anisandrus dispar* galleries were observed, thus making this species unsuitable for colonization success analysis.

X. crassiusculus had the highest incidence in boring activity and colonization success, followed by *X. saxesenii* and *X. germanus*, with significantly lower incidence in both boring activity and colonization success. *A. dispar* dug only 10 galleries out of 2318 total.

Boring activity and colonization pattern differed among ambrosia beetle species and were influenced by the host tree species. Trees in the Rosales group (*M. sylvestris*, *P. armeniaca*, *P. avium* and *P. pyraster*) were generally more subjected to boring activities, and in all four tree species, positive ratios of colonization success were registered for all insect species considered (*X. crassiusculus*, *X. saxesenii*, *X. germanus*).

Trees in the Fagales group (*C. avellana*, *C. betulus*, *Q. ilex*, *Q. robur*) were generally less subjected to boring activities, but the colonization pattern was influenced by the tree species. *C. avellana* and *C. betulus* were proven to be the least preferred and colonized tree species by all the insect species, while *Q. ilex* and *Q. robur* were shown to be preferred by some insect species over others.

Inside the wood, straight and curved galleries were mostly very short, while branched galleries have come in a wide variety of different shapes and sizes: some were composed of a main gallery with shorter ramifications on the sides, while others created complex patterns of multiple ramifications.

Some of the branched galleries presented wide flat brood chambers. In most of the cases, the gallery networks were dug horizontally, with all the ramifications aligned on the same level, while brood chambers were dug vertically, following the direction of the gallery. Several crossed galleries were observed, both between tunnels dug by the same species or by different ones. Cases of galleries originating from inside other galleries were also observed.

4.2. Mean number of entry holes and successful galleries

Boring activity incidence differed among ambrosia beetle species (Fig. 4.36): *X. crassiusculus* (39.71 ± 7.66) scored the highest value, while *X. saxesenii* (10.68 ± 2.20) and *X. germanus* (10.34 ± 2.05), scored similar results compared to each other, but almost 4 times lower than *X. crassiusculus*.

Colonization pattern differed among ambrosia beetle species (Fig. 4.37) and reflected the same trend observed for boring incidence (Fig. 4.36): *X. crassiusculus* (15.42 ± 4.23) scored again the highest value, and *X. saxesenii* (2.21 ± 0.77) and *X. germanus* (1.18 ± 0.36), scored lower results compared to *X. crassiusculus*, with an even greater difference.

Compared to the other insect species, *A. dispar* scored a significantly lower value both in boring incidence (0.26 ± 0.14) and colonization success (0.18 ± 0.14), its presence was observed only in 5 out of 8 tree species (*C. avellana, M. sylvestris, P. avium, P. pyraster, Q. ilex*) and for a total number of 10 out of 2318 galleries, thus making this species unsuitable for further analysis.

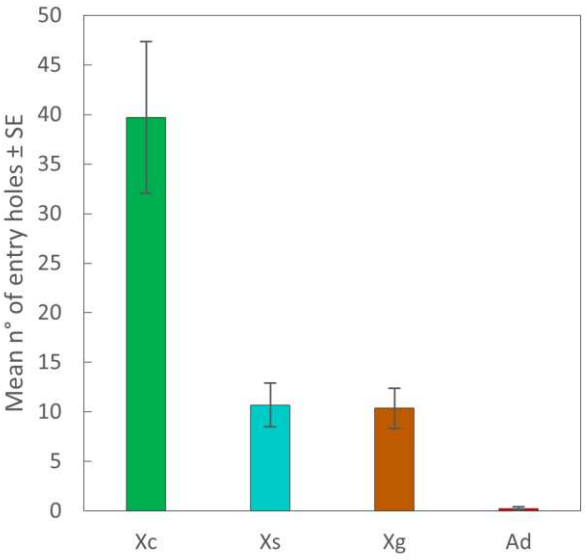

Figure 4.36. Mean number of entry holes, over all the logs, divided by insect species.

Xc = *Xylosandrus crassiusculus*
Xs = *Xyleborinus saxesenii*
Xg = *Xylosandrus germanus*
Ad = *Anisandrus dispar*

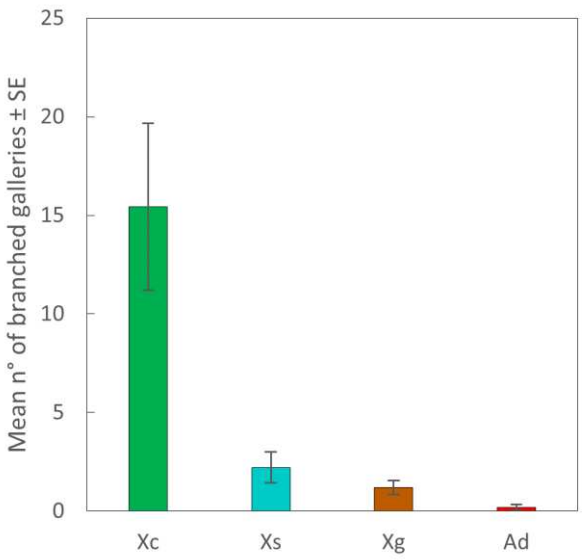

Figure 4.37. Mean number of branched galleries, over all the logs, divided by insect species.

Xc = *Xylosandrus crassiusculus*
Xs = *Xyleborinus saxesenii*
Xg = *Xylosandrus germanus*
Ad = *Anisandrus dispar*

4.3. Plant-host effect on the number of entry holes

Across all the 3 insect species, *M. sylvestris* and *P. armeniaca* were the most attacked tree species, reaching the highest or the second highest average number of entry holes for all the insect species, together with *P. avium* being the third or fourth highest (Fig. 4.38, 4.39, 4.40). Table 4.1 shows statistical indices related to boring activity results presented in Fig. 4.38, 4.39, 4.40.

The most attacked tree species by *X. crassiusculus* were PAR (112.25 ± 5.20), MC (105.60 ± 13.19) and PP (44.20 ± 22.23), followed by PAV (26.40 ± 17.10) and QI (16.25 ± 3.71), and finally CA (9.20 ± 6.11), QR (7.60 ± 2.71) and CB (6.00 ± 4.34). Estimated marginal means show that PAV and QI values share statistical similarities with all the other tree species, while PAR and MC are shown to be different from CA, QR and CB (Fig. 4.38).

The most attacked tree species by *X. saxesenii* were PAR (27.00 ± 6.15), MC (21.00 ± 8.25) and PAV (18.60 ± 7.51), followed by QI (8.50 ± 3.50), PP (6.80 ± 4.84) and CA (3.80 ± 1.88), and finally QR (2.20 ± 0.97) and CB (0.40 ± 0.40). Estimated marginal means show that PP and CA share statistical similarities with all the other tree species, while PAR, MC and PAV are shown to be different from CB and QR (Fig. 4.39).

The most attacked tree species by *X. germanus* were MC (25.80 ± 9.56) and PAR (22.75 ± 7.95), followed by PAV (11.00 ± 2.02), QI (8.50 ± 4.19), QR (6.00 ± 3.21) and CB (5.40 ± 2.50), and finally PP (3.60 ± 1.33) and CA (1.80 ± 1.11). Estimated marginal means show that PAV, QI, QR and CB share statistical similarities with all the other tree species, while PAR and MC are shown to be different from PP and CA (Fig. 4.40).

Considering the results reported in this analysis and the comparisons observed through estimated marginal means, a difference exists between the results achieved in trees among the Rosales group and the ones among the Fagales group. In particular PAR and MC, and also PAV for *X. saxesenii*, all belonging to the Rosales, were shown to be different from CA, QR or CB, which belong to the Fagales group. QI and PP reported similarities with other tree species belonging to different groups or presented no substantial difference with other tree species.

Insect species	**LR Chisq**	**Df**	**Pr(>Chisq)**
X. crassiusculus	46.901	7	0.00005836
X. saxesenii	38.313	7	0.002642
X. germanus	34.684	7	0.01282

Table 4.1. Statistical indices for *X. crassiusculus, X. saxesenii* and *X. germanus* boring activity, showing Likelihood Ratio Chi-square [LR Chisq], Degrees of freedom [Df] and P value [Pr(>Chisq)].

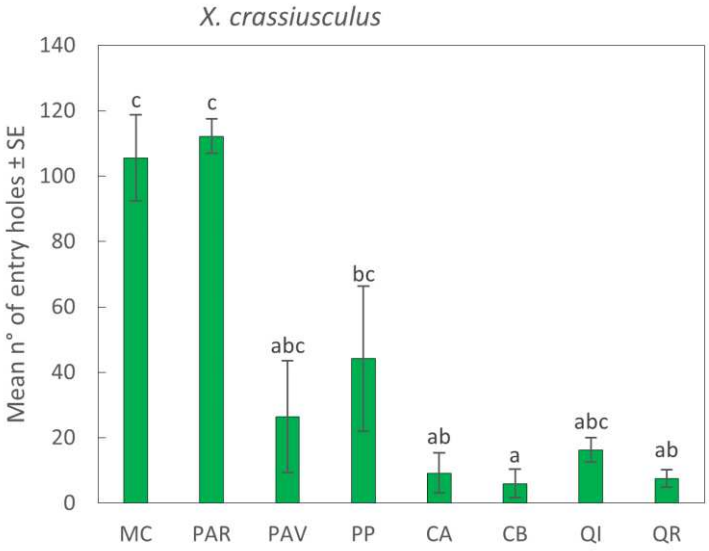

Figure 4.38. Mean number of entry holes of *X. crassiusculus* for each attacked tree species. Estimated marginal means are represented as letters above each tree species. Means with the same letters are proven to not be statistically different. On the left, the tree species in the Rosales group (*M. sylvestris*, *P. armeniaca*, *P. avium* and *P. pyraster*); on the right, the tree species in the Fagales group (*C. avellana*, *C. betulus*, *Q. ilex*, *Q. robur*).

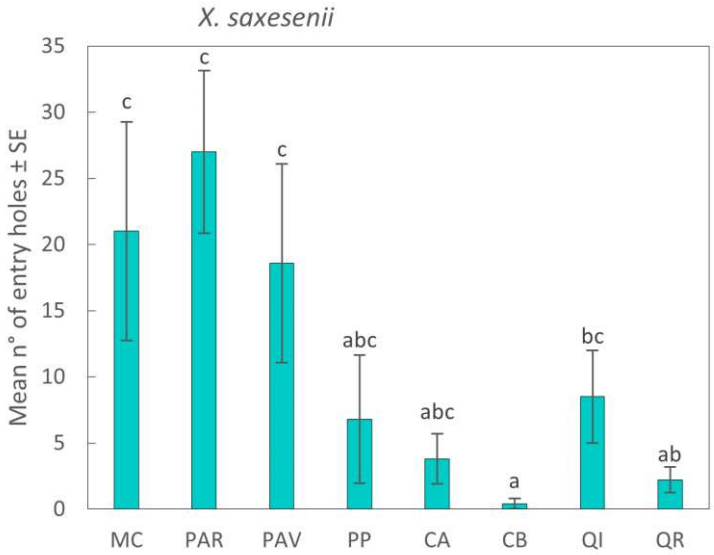

Figure 4.39. Mean number of entry holes of *X. saxesenii* for each attacked tree species. Estimated marginal means are represented as letters above each tree species. Means with the same letters are proven to not be statistically different. On the left, the tree species in the Rosales group (*M. sylvestris*, *P. armeniaca*, *P. avium* and *P. pyraster*); on the right, the tree species in the Fagales group (*C. avellana*, *C. betulus*, *Q. ilex*, *Q. robur*).

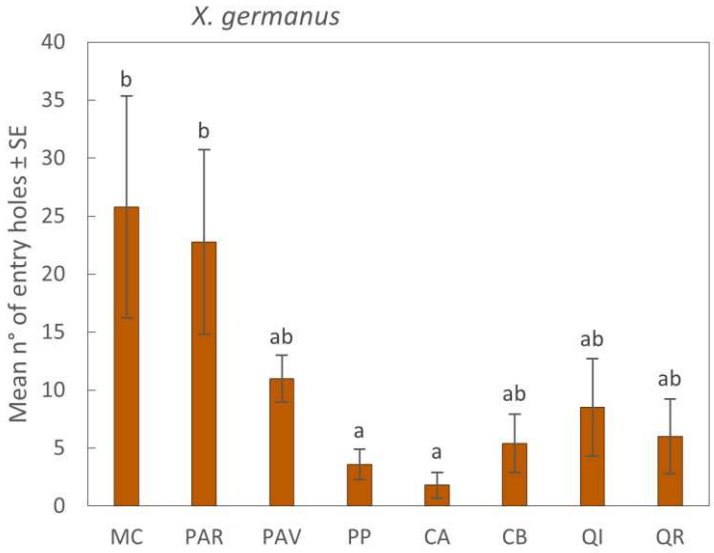

Figure 4.40. Mean number of entry holes of *X. germanus* for each attacked tree species. Estimated marginal means are represented as letters above each tree species. Means with the same letters are proven to not be statistically different. On the left, the tree species in the Rosales group (*M. sylvestris*, *P. armeniaca*, *P. avium* and *P. pyraster*); on the right, the tree species in the Fagales group (*C. avellana*, *C. betulus*, *Q. ilex*, *Q. robur*).

4.4. Colonization success ratio per tree species

Fig. 4.41 shows the average percentage of branched galleries over the total number of galleries within each tree species dug by each insect species. Fig. 4.42, 4.43, 4.44 show colonization success ratios individually for every insect species, but only Fig. 4.42 for *X. crassiusculus* shows grouping symbols (letters a, b, c) for estimated marginal means, as the results for *X. saxesenii and X. germanus* composed a statistical sample too small for this analysis. Tables 4.2, 4.3, 4.4 show statistical indices related to colonization success results presented in Fig. 4.41, 4.42, 4.43, 4.44.

Among all the tree species, *P. avium* and *P. armeniaca* reached the highest colonization success ratios for all the insect species, while *Q. robur* showed a relevant colonization success ratio only for *X. germanus*. No galleries dug in *C. betulus* were reported as successful for any insect species.

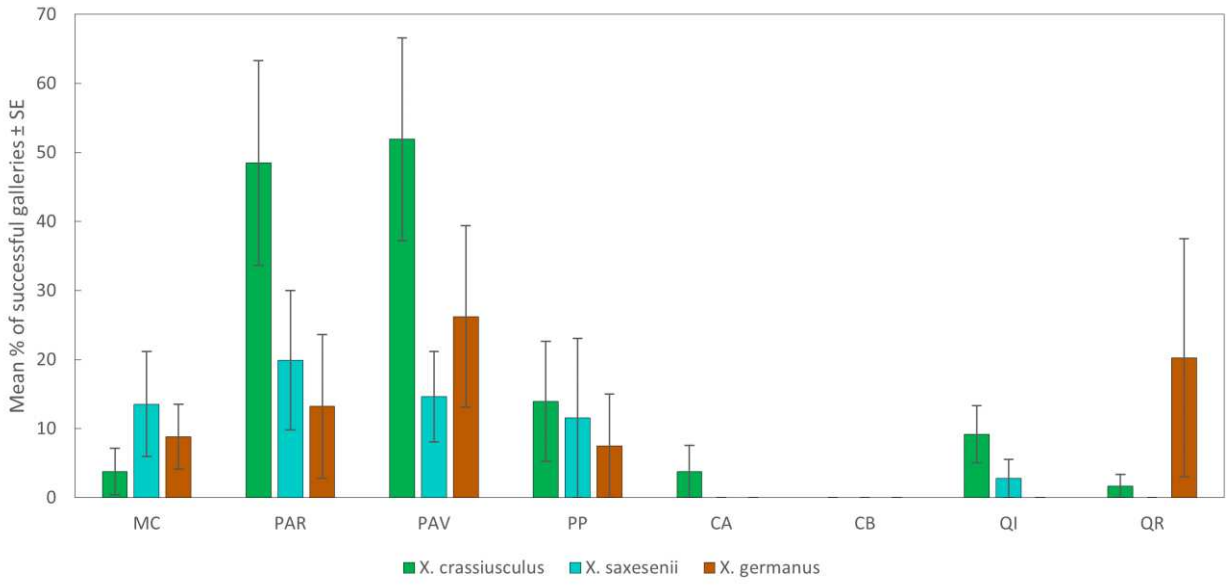

Figure 4.41. Mean percentage of branched galleries for every insect species in every tree species. On the left, the tree species in the Rosales group (*M. sylvestris*, *P. armeniaca*, *P. avium* and *P. pyraster*); on the right, the tree species in the Fagales group (*C. avellana*, *C. betulus*, *Q. ilex*, *Q. robur*).

X. crassiusculus	Df	Sum Sq	Mean Sq	F value	Pr(>F)
Tree_species	7	14635	2090.76	48.063	0.001295
Residuals	27	11745	435.01		

Table 4.2. Statistical indices for *X. crassiusculus*, showing Degrees of freedom [Df], sum squared error [Sum Sq], mean squared error [Mean Sq], F value and P value [Pr(>F)].

X. saxesenii	Df	Sum Sq	Mean Sq	F value	Pr(>F)
Tree_species	7	1521.1	217.30	0.9324	0.5026
Residuals	21	4894.4	233.07		

Table 4.3. Statistical indices for *X. saxesenii*, showing Degrees of freedom [Df], sum squared error [Sum Sq], mean squared error [Mean Sq], F value and P value [Pr(>F)].

X. germanus	Df	Sum Sq	Mean Sq	F value	Pr(>F)
Tree_species	4	1197.7	299.43	0.6284	0.6488
Residuals	17	8099.8	476.46		

Table 4.4. Statistical indices for *X. germanus*, showing Degrees of freedom [Df], sum squared error [Sum Sq], mean squared error [Mean Sq], F value and P value [Pr(>F)].

Colonization success was influenced by the tree species. Each insect species reached positive success ratios of colonization over the four tree species in the Rosales group, while the four species in the Fagales group have proven to exert a stronger selectivity on colonization success of each insect species, with several cases of complete unsuccess where no branched galleries were observed, and other cases of exceptionally high ratios of success for individual insect species.

The success ratios for each species colonized by *X. crassiusculus* are unevenly distributed, but positive for 7 out of 8 tree species (Fig. 4.42). PAV (51.92% ± 14.67%) and PAR (48.97% ± 14.84%) show the highest percentage of colonization success rate, followed by PP (13.93% ± 8.69%), QI (9.20% ± 4.12%), MC (3.79% ± 3.39%), CA (3.79% ± 3.79%) and QR (1.67% ± 1.67%) with a significantly lower colonization success rate. CB was the only tree species where *X. crassiusculus* dug no branched galleries. Estimated marginal means show that MC, QI and PP share statistical similarities with all the other tree species, while PAV is shown to be different from CA, CB and QR.

The success ratios for each species colonized by *X. saxesenii* are evenly distributed among PAR (19.91% ± 10.12%), PAV (14.62% ± 6.56%), MC (13.56% ± 7.62%) and PP (11.54% ± 11.54%), while QI (2.78% ± 2.78%) ratio is significantly lower (Fig. 4.43). CA, CB and QR have shown no branched galleries for *X. saxesenii*.

The success ratios for each species colonized by *X. germanus* are unevenly distributed among PAV (26.23% ± 13.15%), QR (20.27% ± 17.23%), PAR (13.21% ± 10.40%), MC (8.83% ± 4.67%), and PP (7.50% ± 7.50%). CA, CB and QI have shown no branched galleries for *X. germanus* (Fig. 4.44).

Considering the results reported in this analysis, a difference exists between the results achieved in trees among the Rosales group and the ones among the Fagales group, as every insect species was proven to be able to colonize successfully all the tree species among the Rosales group, while only *X. crassiusculus* achieved positive results in 3 out of 4 tree species among the Fagales group, and only *Quercus* spp. reported positive results for *X. saxesenii* and *X. germanus*.

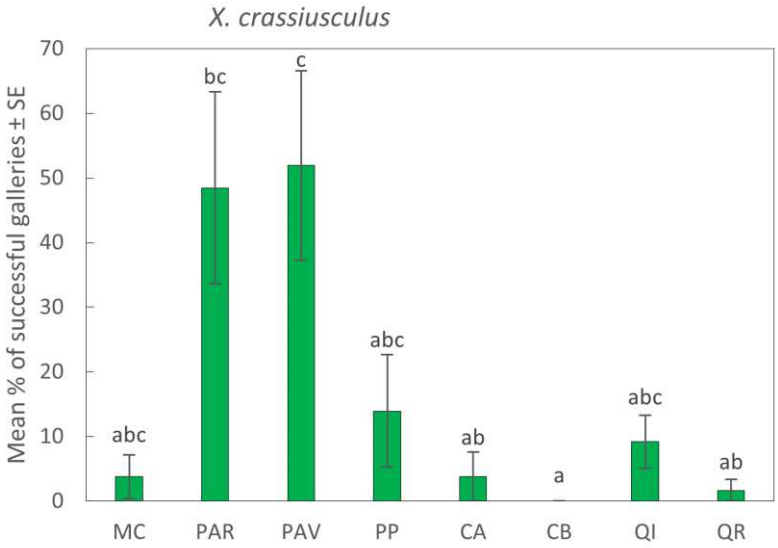

Figure 4.42. Mean percentage of branched galleries of *X. crassiusculus* for each attacked tree species. Estimated marginal means are represented as letters above each tree species. Means with the same letters are proven to not be statistically different. On the left, the tree species in the Rosales group (*M. sylvestris*, *P. armeniaca*, *P. avium* and *P. pyraster*); on the right, the tree species in the Fagales group (*C. avellana*, *C. betulus*, *Q. ilex*, *Q. robur*).

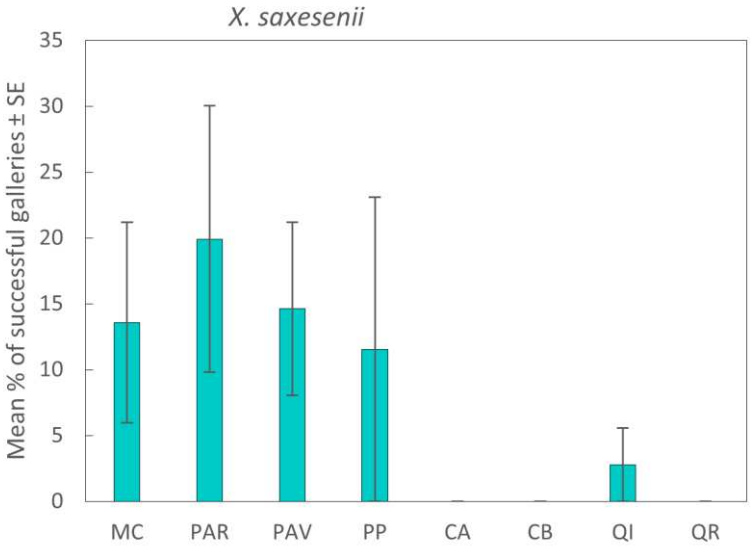

Figure 4.43. Mean percentage of branched galleries of *X. saxesenii* for each attacked tree species. On the left, the tree species in the Rosales group (*M. sylvestris*, *P. armeniaca*, *P. avium* and *P. pyraster*); on the right, the tree species in the Fagales group (*C. avellana*, *C. betulus*, *Q. ilex*, *Q. robur*).

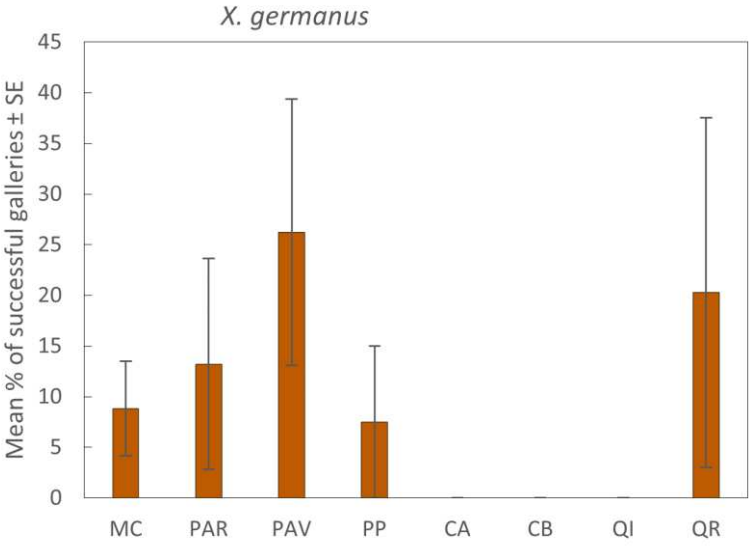

Figure 4.44. Mean percentage of branched galleries of *X. germanus* for each attacked tree species. On the left, the tree species in the Rosales group (*M. sylvestris*, *P. armeniaca*, *P. avium* and *P. pyraster*); on the right, the tree species in the Fagales group (*C. avellana*, *C. betulus*, *Q. ilex*, *Q. robur*).

5. DISCUSSION

To improve management strategies for native and non-native ambrosia beetle species introduced outside their native range, it is necessary to understand all the factors that affect host selection and colonization patterns (Ranger et al., 2016; Cavalletto et al., 2022; Hulcr & Skelton, 2023).

Ethanol constitutes an olfactory cue for several species of ambrosia beetles in locating suitable hosts to colonize and enhance the growth of their nutritional fungal symbionts, favouring trees containing certain ethanol concentrations over others (Ranger et al., 2012, 2015b; Rassati et al., 2020; Cavalletto et al., 2021, 2022).

X-ray tomography has been proven to be an accurate instrument in research to investigate wood-boring insects' activities and cryptic lifestyles in a non-disruptive way (Himmi et al. 2014, 2016a, 2016b, 2018; Aguilera-Olivares et al., 2017; Donkò et al., 2022), and its application to ambrosia beetles have been suggested and supported (Alba-Alejandre et al., 2018; Dolinko et al., 2022), but never attempted before.

The results of this work show a higher incidence of boring activity and colonization success for *X. crassiusculus* over the other insect species, suggesting good performances of this species on flooded trees. On the other hand, results for *A. dispar* suggest an opposite trend, scoring the lowest incidence of boring activity and the lowest presence of developed galleries.

In previous research, *X. crassiusculus* was proven to be effective in boring initiation and colonization at different ethanol concentrations, while *A. dispar* was proven to be positively influenced by increasing concentration of ethanol (Cavalletto et al., 2021, 2022). Both these insect species seem to use ethanol as a main olfactory cue to select their host, with their fungal symbionts being more efficient at different ethanol concentrations, as *A. roeperi* for *X. crassiusculus* has a lower ethanol tolerance than *A. hartigii* for *A. dispar* (Ranger et al., 2018; Lehenberger et al., 2021; Cavalletto et al., 2022).

This explains the attitude of *X. crassiusculus* to attack trees in both early and advanced physiological stress stages, making it a major pest in orchards and tree nurseries (Ranger et al., 2016, 2021), and also explains the opposite preference for *A. dispar* to attack dying or severely stressed trees (Klimetzek et al., 1986; Schroeder & Lindelöw, 1989).

Trees subjected to flooding have relatively low ethanol concentration levels, being in the early stages of physiological stress, thus becoming more attractive for *X. crassiusculus* than for *A. dispar*. The results in this thesis support the hypothesis that ethanol plays a major role in the host selection mechanism for these two insect species, thus regulating niche partitioning among ambrosia beetles (Rassati et al., 2020; Cavalletto et al., 2021, 2022).

The intermediate results achieved by *X. saxesenii* and *X. germanus* can be also explained by the relatively low concentration of ethanol in flooded trees. In previous research, ethanol concentration was proven to influence *X. saxesenii* and *X. germanus* boring activity, with an increasing incidence at higher concentrations, but not the colonization success, which may require the interplay of both ethanol and other olfactory cues (Cavalletto et al., 2021, 2022).

The results of this work show that colonization success is higher for *X. saxesenii* than for *X. germanus*, which is the opposite trend observed by Rassati et al. (2020). This may enforce the hypothesis that, for both *X. saxesenii* and *X. germanus*, compounds other than ethanol may influence colonization success, such as quercivorol or α–copaene (Owens et al., 2019).

Considering the relationship between each tree species and the ambrosia beetle species analysed, different patterns are revealed. The difference between trees among the Rosales and the ones among the Fagales is clear for both boring incidence and colonization success, as the trees in the first group reported sensibly higher values than trees in the second group.

The reason why trees in the Rosales group are more sensible to attacks of ambrosia beetles than trees in the Fagales may be related to the plant resistance to flooding stress, which may lead to different emission levels of ethanol and other stress-related compounds (Copolovici & Niinemets, 2010).

Among the eight tree species present in this work, *P. avium* and *P. armeniaca*, in the Rosales group, are the most sensitive species to flood stress (Glenz et al., 2006; Ranney et al., 1994), thus producing the highest amount of ethanol when subjected to flooding. In fact, *P. armeniaca* was the most or the second most attacked and colonized species for all three insect species, while *P. avium* reported high boring activity and colonization success for *X. saxesenii* and the highest colonization success for *X. crassiusculus* and *X. germanus*.

The other two species in this group reported different trends. *M. sylvestris* was one of the most attacked tree species overall, indicating high levels of ethanol emitted, but the colonization success

ratio was unexpectedly low compared to *P. armeniaca* and *P. avium* for *X. germanus* and *X. crassiusculus*, highlighting the interplay of factors other than ethanol that influence colonization success of these species. *P. pyraster* reported an overall low incidence of boring activity and colonization success ratios, as this tree species is considered resistant to flood stress (Vidaković et al., 2022; Glenz et al., 2006), thus emitting a lower concentration of ethanol.

On the other hand, among the Fagales group, *C. avellana* and *C. betulus* reported the lowest incidence of boring activity and colonization success ratios almost null, with only *X. crassiusculus* being able to establish a few developed galleries in *C. avellana*.

The other two tree species, however, reported unexpected results. *Q. ilex* reported the highest boring activity among Fagales, with an incidence similar to Rosales. This may be related to the low tolerance of this tree species to flooding stress, which caused the emission of higher concentrations of ethanol (Holzinger et al., 2000) and attracted more insects. However, colonization success was null for *X. germanus* and significant only for *X. crassiusculus*, with lower ratios for *X. saxesenii*.

Q. robur reported a low incidence of boring activity among all insect species, and colonization success was null for *X. crassiusculus and X. saxesenii*, but exceptionally higher for *X. germanus*. This tree species has moderate resistance to flooding (Glenz et al., 2006), so factors other than ethanol concentration must be involved in colonization success, which is in line with previous research on this insect species (Cavalletto et al., 2022).

All the results suggest that flooding may affect differently the eight tree species involved in this research, with the Rosales group being more sensitive than Fagales to flooding stress. Ethanol is confirmed to be the main attracting cue for ambrosia beetle species, driving host selection mechanisms and regulating niche partitioning among the insect species.

However, colonization success is proven to be affected not only by ethanol emissions, which increase with lower flooding stress tolerance of the plant, but also by other unclear factors related to specific insect species, with *X. crassiusculus* being able to colonize almost all the analysed tree species, and *X. germanus* reporting high colonization success ratios in *Q. robur*, which is a flood-resistant tree species.

6. CONCLUSIONS

X-ray tomography is an essential instrument to study wood-boring beetles such as ambrosia beetles, unravelling the mysteries of their cryptic lifestyles and allowing deep and detailed comprehension of their ecology and biology.

The observation of the complex gallery systems dug by these insects opens new frontiers for research on their social behaviour, gallery structure, interactions among different species and much more.

This research has remarked on the importance of ethanol in the plant-host relationship, affecting the host selection mechanism and the colonization success of ambrosia beetles.

Through the observation of the galleries dug by ambrosia beetles, it was proven that flooding stress affected differently the incidence of boring activities of ambrosia beetles and their colonization success, with trees among the Rosales being attacked more frequently than trees among the Fagales.

Tree species in the Rosales group are common in tree nurseries and orchards, which are intensively managed environments where poor drainage of the soil is a recurrent condition, posing a major threat for possible ambrosia beetle attacks.

Management strategies in these environments should be focused on keeping plants in good health conditions, as ambrosia beetles are proven to be ineffective on healthy trees.

However, both natural and intensively managed forest environments may face increasing levels of ambrosia beetles' attacks in the future, due to climate change that will inevitably raise the frequency of flooding events all over the world.

Considering this trend, research on these insects is becoming more and more relevant to understand their behaviour, monitor their presence, and manage them when they become pests, especially exotic species such as *X. crassiusculus*, that is highly adaptable on several different tree species and conditions and has already posed a major threat for orchards and tree nurseries in the US.

ACKNOWLEDGEMENTS

I would like to express my deepest gratitude to Giacomo Cavalletto, for his availability and the support he provided me for the technical execution of the analysis work, and his wise and careful advice on the development of this research, this endeavour would not have been possible without his help.

I am also grateful to Nicolò Trevisan for the help and suggestions they gave me in using Blender 3.5, essential to carry out this work.

I would like to extend my sincere thanks to Luisa Scabbio, my dear aunt, for the beautiful photos we took together, which enriched this work with marvellous and clear images.

I'd like to acknowledge all the work carried out by Francesca Carloni, a dear friend of mine, in her master's thesis, which preceded this thesis work and provided important information for this research.

Many thanks to Professor Andrea Battisti who introduced me to this project, for his availability and kindness in guiding me to find a thesis project to work on that reflected my interests.

I would be remiss in not mentioning Luca Deganutti, a dear friend of mine who accompanied me throughout my studies, and who always has been available when I needed.

Lastly, I'd like to mention all the people who followed and supported me throughout my studies and for this thesis project. My dear colleagues and friends who supported me through my studies: Lazhari Chater, Shyam Praveen Rajendran, Francesco Piccinin, Francesca Moraldo, Claudio Romano, Giacomo Visentin, Massimo Ceolato and Filippo Biscontin. My family, for the immense and unconditional support throughout my studies to the end: Rosanna Rosada, Mauro Scabbio, Annachiara Scabbio, Sara Scabbio, Silvana Florian, Emanuela Rosada, Luigi Silvestrini, Mattia Silvestrini, Linda Silvestrini, Laura Scabbio, Luisa Scabbio, Fabio Scantamburlo, Daniele Scantamburlo and Giorgia Scantamburlo. My dear friends and companions in all my adventures and journeys, who always have been by my side since our childhood: Luca Guernier and Nicolò Giacchetto. And finally, my beloved Matteo Zanusso, who always has been close to me since the day we met.

REFERENCES

Aguilera-Olivares, D., Palma-Onetto, V., Flores-Prado, L., Zapata, V., & Niemeyer, H.M. (2017). X-ray computed tomography reveals that intraspecific competition promotes soldier differentiation in a one-piece nesting termite. *Entomologia Experimentalis et Applicata*, **163**(1), 26-34. https://doi.org/10.1111/eea.12557

Alba-Alejandre, I., Alba-Tercedor, J., & Vega, F. E. (2018). Observing the devastating coffee berry borer (Hypothenemus hampei) inside the coffee berry using micro-computed tomography. *Scientific Reports*, **8**(1), 17033. https://doi.org/10.1038/s41598-018-35324-4

Batra, L. R. (1963). Ecology of ambrosia fungi and their dissemination by beetles. *Transactions of the Kansas Academy of Science (1903-)*, **66**(2), 213-236. https://doi.org/10.2307/3626562

Berville, L., Darrouzet, E. (2019). Wood excavation, construction, and architecture in two Reticulitermes subterranean termites. *Insect. Soc.* **66**, 403–411. https://doi.org/10.1007/s00040-019-00696-x

Carloni, F. (2022). *Effects of host trees on colonization patterns by ambrosia beetles under different abiotic stressors* [Master's thesis, Università degli Studi di Padova]. Padua Thesis and Dissertation Archive. https://hdl.handle.net/20.500.12608/37155

Carrillo, D., Duncan, R. E., Ploetz, J. N., Campbell, A. F., Ploetz, R. C., & Peña, J. E. (2014). Lateral transfer of a phytopathogenic symbiont among native and exotic ambrosia beetles. *Plant Pathology*, **63**(1), 54-62. https://doi.org/10.1111/ppa.12073

Cavaletto, G., Faccoli, M., Ranger, C. M., & Rassati, D. (2021). Ambrosia beetle response to ethanol concentration and host tree species. *Journal of Applied Entomology*, **145**(8), 800-809. https://doi.org/10.1111/jen.12895

Cavaletto, G., Ranger, C. M., Reding, M. E., Montecchio, L., & Rassati, D. (2022). Species-specific effects of ethanol concentration on host colonization by four common species of ambrosia beetles. *Journal of Pest Science*, **96**(2), 833-843. https://doi.org/10.1007/s10340-022-01537-w

Chen, Y., Coleman, T. W., Ranger, C. M., & Seybold, S. J. (2021). Differential flight responses of two ambrosia beetles to ethanol as indicators of invasion biology: the case with Kuroshio shot hole borer (Euwallacea kuroshio) and fruit-tree pinhole borer (Xyleborinus saxesenii). *Ecological Entomology*, **46**(3), 651-667. https://doi.org/10.1111/een.13013

Choi, B., Himmi, S. K., & Yoshimura, T. (2017). Quantitative observation of the foraging tunnels in Sitka spruce and Japanese cypress caused by the drywood termite Incisitermes minor (Hagen) by 2D and 3D X-ray computer tomography (CT). *Holzforschung*, **71**(6), 535-542. https://doi.org/10.1515/hf-2016-0140

Copolovici, L., & NIINEMETS, Ü. (2010). Flooding induced emissions of volatile signalling compounds in three tree species with differing waterlogging tolerance. *Plant, Cell & Environment*, **33**(9), 1582-1594. https://doi.org/10.1111/j.1365-3040.2010.02166.x

Dole, S. A., Jordal, B. H., & Cognato, A. I. (2010). Polyphyly of Xylosandrus Reitter inferred from nuclear and mitochondrial genes (Coleoptera: Curculionidae: Scolytinae). *Molecular phylogenetics and evolution*, **54**(3), 773-782. https://doi.org/10.1016/j.ympev.2009.11.011

Dolinko, A. E., Costales, Y., Carmarán, C., & Ceriani-Nakamurakare, E. (2022). A novel set of algorithms to recognize galleries of ambrosia beetle in computerized axial tomography of trees trunks. *arXiv preprint arXiv:2206.12748*. https://doi.org/10.48550/arXiv.2206.12748

Donkó, T., Petneházy, Ö., Fajtai, D., & Keszthelyi, S. (2022). A conceptualisation of computed tomography outputs in entomological research by step by step displaying trough the CT-based visualization of a wood-boring larvae. *Acta Phytopathologica et Entomologica Hungarica*, **57**(2), 127-138. https://doi.org/10.1556/038.2022.00148

Dzurenko, M., & Hulcr, J. (2022). Ambrosia beetles. *Current Biology*, **32**(2), R61-R62. https://doi.org/10.1016/j.cub.2021.11.043

Easterling, D. R., Meehl, G. A., Parmesan, C., Changnon, S. A., Karl, T. R., & Mearns, L. O. (2000). Climate extremes: observations, modeling, and impacts. *Science*, **289**(5487), 2068-2074. https://doi.org/10.1126/science.289.5487.2068

Faccoli, M. (2015). Scolitidi d'Europa: tipi, caratteristiche e riconoscimento dei sistemi riproduttivi. European bark and ambrosia beetles: types, characteristics and identification of mating systems. *WBA Handbooks, Verona*.

Fuchs, A., Schreyer, A., Feuerbach, S., & Korb, J. (2004). A new technique for termite monitoring using computer tomography and endoscopy. *International Journal of Pest Management*, **50**(1), 63-66. https://doi.org/10.1080/0967087032000159300

Galko, J., Dzurenko, M., Ranger, C. et al. (2019). Distribution, habitat preference, and management of the invasive ambrosia beetle Xylosandrus germanus (Coleoptera: Curculionidae, Scolytinae) in European forests with an emphasis on the west Carphatians. *Forests*, **10**, 10. https://doi.org/10.3390/f10010010

Glenz, C., Schlaepfer, R., Iorgulescu, I., & Kienast, F. (2006). Flooding tolerance of Central European tree and shrub species. *Forest Ecology and Management*, **235**(1-3), 1-13. https://doi.org/10.1016/j.foreco.2006.05.065

Harit, A. K., Ramasamy, E. V., Babu, N., Rajasree, M. J., Monsy, P., Bottinelli, N., Cheik, S., & Jouquet, P. (2021). Are wood-feeding and fungus-growing termites so different? Comparison of the organization and properties of Microcerotermes pakistanicus and Odontotermes obesus soil constructions in the Western Ghats, India. *Insectes Sociaux*, **68**(2-3), 207-216. https://doi.org/10.1007/s00040-021-00818-4

Himmi, S. K., Yoshimura, T., Yanase, Y., Oya, M., Torigoe, T., & Imazu, S. (2014). X-ray tomographic analysis of the initial structure of the royal chamber and the nest-founding behavior of the drywood termite Incisitermes minor. *Journal of wood science*, **60**, 453-460. https://doi.org/10.1007/s10086-014-1427-x

Himmi, S. K., Yoshimura, T., Yanase, Y., Mori, T., Torigoe, T., & Imazu, S. (2016a). Wood anatomical selectivity of drywood termite in the nest-gallery establishment revealed by X-ray tomography. *Wood science and technology*, **50**, 631-643. https://doi.org/10.1007/s00226-016-0800-x

Himmi, S. K., Yoshimura, T., Yanase, Y., Oya, M., Torigoe, T., Akada, M., & Imadzu, S. (2016b). Nest-gallery development and caste composition of isolated foraging groups of the drywood termite, Incisitermes minor (Isoptera: Kalotermitidae). *Insects*, **7**(3), 38. https://doi.org/10.3390/insects7030038

Himmi, S. K., Yoshimura, T., Yanase, Y., Torigoe, T., Akada, M., Ikeda, M., & Imazu, S. (2018). Volume visualization of hidden gallery system of drywood termite using computed tomography: a new approach on monitoring of termite infestation. *Sustainable future for human security: environment and resources*, 61-68. https://doi.org/10.1007/978-981-10-5430-3_6

Hoffmann, C. H. (1941). Biological observations on Xylosandrus germanus (Bldfd.). *Journal of Economic Entomology*, **34**(1). https://doi.org/10.1093/jee/34.1.38

Holzinger, R., Sandoval-Soto, L., Rottenberger, S., Crutzen, P. J., & Kesselmeier, J. (2000). Emissions of volatile organic compounds from Quercus ilex L. measured by Proton Transfer Reaction Mass Spectrometry under different environmental conditions. *Journal of Geophysical Research: Atmospheres*, **105**(D16), 20573-20579. https://doi.org/10.1029/2000JD900296

Hulcr, J., Mogia, M., Isua, B., & Novotny, V. (2007). Host specificity of ambrosia and bark beetles (Col., Curculionidae: Scolytinae and Platypodinae) in a New Guinea rainforest. *Ecological Entomology*, **32**(6), 762-772. https://doi.org/10.1111/j.1365-2311.2007.00939.x

Hulcr, J., Atkinson, T. H., Cognato, A. I., Jordal, B. H., & McKenna, D. D. (2015). Morphology, taxonomy, and phylogenetics of bark beetles. In Vega FE, Hofstetter RW (eds) *Bark beetles: biology and ecology of native and invasive species* (pp. 41-84). Academic Press. https://doi.org/10.1016/B978-0-12-417156-5.00002-2

Hulcr, J., Black, A., Prior, K., Chen, C. Y., & Li, H. F. (2017). Studies of ambrosia beetles (Coleoptera: Curculionidae) in their native ranges help predict invasion impact. *Florida Entomologist*, **100**, 257–261. https://doi.org/10.1653/024.100.0219

Hulcr, J., & Stelinski, L. L. (2017). The ambrosia symbiosis: from evolutionary ecology to practical management. *Annual review of entomology*, **62**, 285-303. https://doi.org/10.1146/annurev-ento-031616-035105

Hulcr, J., & Skelton, J. (2023). Ambrosia Beetles. In: D. Allison, J., Paine, T.D., Slippers, B., Wingfield, M.J. (eds) *Forest Entomology and Pathology*. Springer, Cham. https://doi.org/10.1007/978-3-031-11553-0_11

Jennings, J. T., & Austin, A. D. (2011). Novel use of a micro-computed tomography scanner to trace larvae of wood boring insects. *Australian journal of entomology*, **50**(2), 160-163. https://doi.org/10.1111/j.1440-6055.2010.00792.x

Kamata, N., Esaki, K., Mori, K., Takemoto, H., Mitsunaga, T., & Honda, H. (2008). Field trap test for bioassay of synthetic (1 S, 4 R)-4-isopropyl-1-methyl-2-cyclohexen-1-ol as an aggregation pheromone of Platypus quercivorus (Coleoptera: Platipodidae). *Journal of forest research*, **13**, 122-126. https://doi.org/10.1007/s10310-007-0053-5

Kendra, P. E., Owens, D., Montgomery, W. S., Narvaez, T. I., Bauchan, G. R., Schnell, E. Q., Tabanca, N., & Carrillo, D. (2017). α-Copaene is an attractant, synergistic with quercivorol, for improved detection of Euwallacea nr. fornicatus (Coleoptera: Curculionidae: Scolytinae). *PLoS One*, **12**(6), e0179416. https://doi.org/10.1371/journal.pone.0179416

Kelsey, R. G., Beh, M. M., Shaw, D. C., & Manter, D. K. (2013). Ethanol attracts scolytid beetles to Phytophthora ramorum cankers on coast live oak. *Journal of Chemical Ecology*, **39**, 494–506. https://doi.org/10.1007/s1088 6-013-0271-6

Kelsey, R. G., Gallego, D., Sanchez-Garcia, F. J., & Pajares, J. A. (2014). Ethanol accumulation during severe drought may signal tree vulnerability to detection and attack by bark beetles. *Canadian Journal of Forest Research*, **44**, 554–561. https://doi.org/10.1139/cjfr-2013-0428

Kharin, V. V., & Zwiers, F. W. (2005). Estimating extremes in transient climate change simulations. *Journal of Climate*, **18**(8), 1156-1173. https://doi.org/10.1175/JCLI3320.1

Kirkendall, L. R. (1993). Ecology and evolution of biased sex ratios in bark and ambrosia beetles. *Evolution and diversity of sex ratio in insects and mites.*, 235-345.

Kirkendall, L. R., Biedermann, P. H., & Jordal, B. H. (2015). Evolution and diversity of bark and ambrosia beetles, pp. 85–156. In F. E. Vega and R. W. Hofstetter (eds.), *Bark Beetles: Biology and Ecology of Native and Invasive Species*. Elsevier, London, United Kingdom. https://doi.org/10.1016/B978-0-12-417156-5.00003-4

Klimetzek, D., Kohler, J., Vite, J. P., & Kohnle, U. (1986). Dosage response to ethanol mediates host selection by "secondary" bark beetles. *Naturwissenschaften*, **73**, 270–272. https://doi.org/10.1007/BF00367783

La Spina, S., De Canniere, C., Dekri, A., & Gregoire, J. C. (2013). Frost increases beech susceptibility to scolytine ambrosia beetles. Agricultural and Forest Entomology, 15, 157–167. https://doi.org/10.1111/j.1461-9563.2012.00596.x

Lehenberger, M., Benkert, M., & Biedermann, P. B. (2021). Ethanol-enriched substrate facilitates ambrosia beetle fungi, but inhibits their pathogens and fungal symbionts of bark beetles. Frontiers in Microbiology, 11, 590111. https://doi.org/10.3389/fmicb.2020.590111

Manion, P. D. (1981). *Tree disease concepts*. Prentice-Hall, Inc..

McPherson, B. A., Erbilgin, N., Wood, D. L., Svihra, P., Storer, A. J., & Standiford, R. B. (2008). Attraction of ambrosia and bark beetles to coast live oaks infected by Phytophthora ramorum. *Agricultural and Forest Entomology*, **10**, 315–321. https://doi.org/10.1111/j.1461-9563.2008.00386.x

Nahirney, P. C., Forbes, J. G., Douglas Morris, H., Chock, S. C., & Wang, K. (2006). What the buzz was all about: superfast song muscles rattle the tymbals of male periodical cicadas. *The FASEB journal*, **20**(12), 2017-2026. https://doi.org/10.1096/fj.06-5991com

Normark, B. B., Jordal, B. H., & Farrell, B. D. (1999). Origin of a haplodiploid beetle lineage. Proceedings of the Royal Society of London. *Series B: Biological Sciences*, **266**(1435), 2253-2259. https://doi.org/10.1098/rspb.1999.0916

Owens, D., Kendra, P. E., Tabanca, N., Narvaez, T. I., Montgomery, W. S., Schnell, E. Q., & Carrillo, D. (2019). Quantitative analysis of contents and volatile emissions from α-copaene and quercivorol lures, and longevity for attraction of Euwallacea nr. fornicatus in Florida. *Journal of Pest Science*, **92**, 237–252. https://doi.org/10.1007/s10340-018-0960-6

Parry M., Canziani O., Palutikof J., van der Linden P. & Hanson C. (eds) (2007) Climate Change 2007 – Impacts, Adaptation and Vulnerability. *Contribution of Working Group II to the Fourth Assessment Report of the IPCC*. Cambridge University Press, New York, NY, USA.

Postnov, A., De Clerck, N., Sasov, A., & Van Dyck, D. (2002). 3D in-vivo X-ray microtomography of living snails. *Journal of Microscopy*, **205**(2), 201-204. https://doi.org/10.1046/j.0022-2720.2001.00986.x

Ranger, C. M., Reding, M. E., Persad, A. B., & Herms, D. A. (2010). Ability of stress-related volatiles to attract and induce attacks by Xylosandrus germanus and other ambrosia beetles (Coleoptera: Curculionidae, Scolytinae). *Agricultural and Forest Entomology*, **12**, 177–185. https://doi.org/10.1111/j.1461-9563.2009.00469.x

Ranger, C. M., Reding, M. E., Schultz, P. B., & Oliver, J. B. (2012). Ambrosia beetle (Coleoptera: Curculionidae) responses to volatile emissions associated with ethanol-injected Magnolia virginiana. *Environmental Entomology*, **41**(3), 636-647. https://doi.org/10.1603/EN11299

Ranger, C. M., Reding, M. E., Schultz, P. B., & Oliver, J. B. (2013). Influence of flood-stress on ambrosia beetle host selection and implications for their management in a changing climate. *Agricultural and Forest Entomology*, **15**, 56–64. https://doi.org/10.1111/j.1461-9563.2012.00591.x

Ranger, C. M., Tobin, P. C., & Reding, M. E. (2015a). Ubiquitous volatile compound facilitates efficient host location by a non-native ambrosia beetle. *Biological Invasions*, **17**, 675-686. https://doi.org/10.1007/s10530-014-0758-2

Ranger, C. M., Schultz, P. B., Frank, S. D., Chong, J. H., & Reding, M. E. (2015b). Non-native ambrosia beetles as opportunistic exploiters of living but weakened trees. *PLoS One*, **10**(7), e0131496. https://doi.org/10.1371/journal.pone.0131496

Ranger, C. M., Reding, M. E., Schultz, P. B., Oliver, J. B., Frank, S. D., Addesso, K. M., Chong, J. H., Sampson, B., Werle, C., Gill, S., & Krause, C. (2016a). Biology, ecology, and management of nonnative ambrosia beetles (Coleoptera: Curculionidae: Scolytinae) in ornamental plant nurseries. *Journal of Integrated Pest Management*, **7**(1), 9. https://doi.org/10.1093/jipm/pmw005

Ranger, C. M., Schultz, P. B., Reding, M. E., Frank, S. D., & Palmquist, D. E. (2016b). Flood stress as a technique to assess preventive insecticide and fungicide treatments for protecting trees against ambrosia beetles. *Insects*, **7**(3), 40. https://doi.org/10.3390/insects7030040

Ranger, C. M., Biedermann, P. H., Phuntumart, V., Beligala, G. U., Ghosh, S., Palmquist, D. E., Mueller, R., Barnett, J., Schultz, P. B., Reding, M. E., & Benz, J. P. (2018). Symbiont selection via alcohol benefits fungus farming by ambrosia beetles. *Proceedings of the National Academy of Sciences*, **115**(17), 4447-4452. https://doi.org/10.1073/pnas.17168 52115

Ranger, C. M., Schultz, P. B., Frank, S. D., & Reding, M. E. (2019). Freeze stress of deciduous trees induces attacks by opportunistic ambrosia beetles. *Agricultural and Forest Entomology*, **21**(2), 168-179. https://doi.org/10.1111/afe.12317

Ranger, C. M., Reding, M. E., Addesso, K., Ginzel, M., & Rassati, D. (2021). Semiochemical-mediated host selection by Xylosandrus spp. ambrosia beetles (Coleoptera: Curculionidae) attacking horticultural tree crops: a review of basic and applied science. *The Canadian Entomologist*, **153**(1), 103-120. https://doi.org/10.4039/tce.2020.51

Rassati, D., Faccoli, M., Battisti, A., & Marini, L. (2016). Habitat and climatic preferences drive invasions of non-native ambrosia beetles in deciduous temperate forests. *Biological Invasions*, **18**, 2809-2821. https://doi.org/10.1007/s10530-016-1172-8

Rassati, D., Contarini, M., Ranger, C. M., Cavaletto, G., Rossini, L., Speranza, S., Faccoli, M., & Marini, L. (2020). Fungal pathogen and ethanol affect host selection and colonization success in ambrosia beetles. *Agricultural and Forest Entomolog*y, **22**(1), 1-9. https://doi.org/10.1111/afe.12351

Rallo, G. (1992) - Bosco Nordio Riserva Naturale Integrale, Provincia di Venezia – *Speciale Aree Protette*, **5 – 6** , 44.

Ranney, T. G. (1994). Differential tolerance of eleven Prunus taxa to root zone flooding. *Journal of Environmental Horticulture*, **12**(3), 138-141. https://doi.org/10.24266/0738-2898-12.3.138

Reding, M. E., & Ranger, C. M. (2020). Attraction of invasive ambrosia beetles (Coleoptera: Curculionidae: Scolytinae) to ethanol-treated tree bolts. *Journal of economic entomology*, **113**(1), 321-329. https://doi.org/10.1093/jee/toz282

Schroeder, L. M., & Lindelöw, Å. (1989). Attraction of scolytids and associated beetles by different absolute amounts and proportions of α-pinene and ethanol. *Journal of Chemical Ecology*, **15**, 807-817. https://doi.org/10.1007/BF01015179

Seibold, S., Müller, J., Allner, S., Willner, M., Baldrian, P., Ulyshen, M. D., Brandl, R., Bässler, C., Hagge, J., & Mitesser, O. (2022). Quantifying wood decomposition by insects and fungi using computed tomography scanning and machine learning. *Scientific reports*, **12**(1), 16150. https://doi.org/10.1038/s41598-022-20377-3

Skelton, J., Johnson, A. J., Jusino, M. A., Bateman, C. C., Li, Y., & Hulcr, J. (2019a). A selective fungal transport organ (mycangium) maintains coarse phylogenetic congruence between fungus-farming ambrosia beetles and their symbionts. *Proceedings of the Royal Society B*, **286**(1894), 20182127. https://doi.org/10.1098/rspb.2018.2127

Skelton, J., Jusino, M. A., Carlson, P. S., Smith, K., Banik, M. T., Lindner, D. L., Palmer, J. M., & Hulcr, J. (2019b). Relationships among wood-boring beetles, fungi, and the decomposition of forest biomass. *Molecular Ecology*, **28**(22), 4971-4986. https://doi.org/10.1111/mec.15263

Skelton, J., Loyd, A., Smith, J. A., Blanchette, R. A., Held, B. W., & Hulcr, J. (2020). Fungal symbionts of bark and ambrosia beetles can suppress decomposition of pine sapwood by competing with wood-decay fungi. *Fungal Ecology*, **45**, 100926. https://doi.org/10.1016/j.funeco.2020.100926

Tarver, M. R., Shade, R. E., Tarver, R. D., Liang, Y., Krishnamurthi, G., Pittendrigh, B. R., & Murdock, L. L. (2006). Use of micro-CAT scans to understand cowpea seed resistance to Callosobruchus maculatus. *Entomologia Experimentalis et Applicata*, **118**(1), 33-39. https://doi.org/10.1111/j.1570-7458.2006.00360.x

Vidaković, A., Šatović, Z., Tumpa, K., Idžojtić, M., Liber, Z., Pintar, V., Radunić, M., Runjić, T. N., Runjić, M., Rošin, J., Gaunt, D., & Poljak, I. (2022). Phenotypic variation in European wild pear (Pyrus pyraster (L.) Burgsd.) populations in the North-Western Part of the Balkan Peninsula. *Plants*, **11**(3), 335. https://doi.org/10.3390/plants11030335

Wang, Z., Li, Y., Ernstsons, A. S., Sun, R., Hulcr, J., & Gao, L. (2021). The infestation and habitat of the ambrosia beetle Euwallacea interjectus (Coleoptera: Curculionidae: Scolytinae) in the riparian zone of Shanghai. *Agricultural and Forest Entomology*. **23**, 104–109. https://doi.org/10.1111/afe.12405

Yang, C. Y., Kim, J., & Kim, K. H. (2018). Benzaldehyde synergizes the response of female Xyleborinus saxesenii (Coleoptera: Curculionidae, Scolytinae) to ethanol. *Journal of Economic Entomology*, **111**, 1691–1695. https://doi.org/10.1093/jee/toy131

Yang, H., Gao, S., Wang, J., Li, W., Hou, Q., & Qiu, J. (2022). Three-dimensional reconstruction of Monochamus alternatus galleries using CT scans. *Insects*, **13**(8), 692. https://doi.org/10.3390/insects13080692

R Core Team (2021). R: a language and environment for statistical computing.

WEBSITES

https://xyleborini.myspecies.info/taxonomy/term/1168

https://xyleborini.myspecies.info/taxonomy/term/1176

https://xyleborini.myspecies.info/taxonomy/term/1219

http://treatment.plazi.org/id/03F2065AF00A2204FF3B9E2EFBB21952

https://xyleborini.myspecies.info/taxonomy/term/179

https://www.scientificamerican.com/article/rising-costs-of-u-s-flood-damage-linked-to-climate-change/

https://www.researchgate.net/figure/Diagram-of-alcoholic-fermentation-pathway-in-plants-Alcoholic-fermentation-occurs-in-two_fig1_249882668

https://www.r-project.org/